Microstructure-Sensitive Crystal Viscoplasticity for Ni-base Superalloys

(with application to long-term creep-fatigue interactions)

Award DE-FE0011722
August 2013 – December 2017 (including NCE)
Program Manager: Dr. Patcharin Burke

PI: Richard W. Neu

The George W. Woodruff School of Mechanical Engineering
School of Materials Science & Engineering
Georgia Institute of Technology
Atlanta, GA 30332-0405
rick.neu@gatech.edu

University Turbine Systems Research Workshop
Pittsburgh
November 1-2, 2017

Hot Section Gas Turbine Materials


Power Output: 375 MW

Land-based gas turbines

- drive to increase service temperature to improve efficiency; increase life; with minimal increase in cost
- replace large directionally-solidified Ni-base superalloys with single crystal superalloys

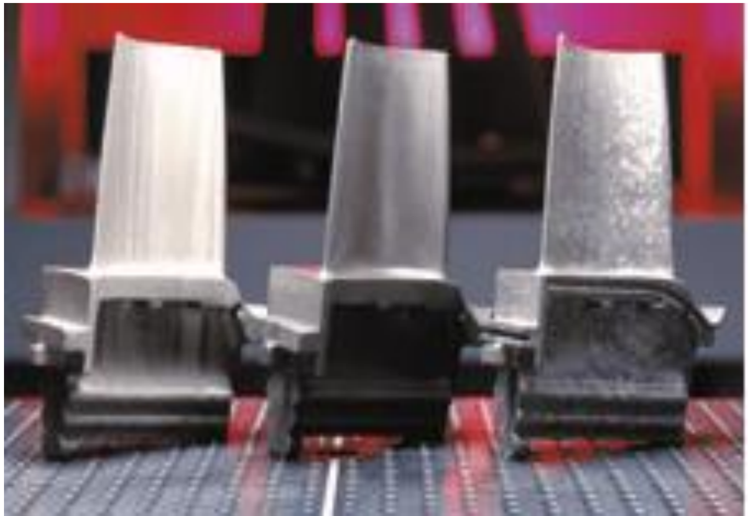

Complexities in evaluating creep-fatigue interaction

[Attari et al., 2013]

[Vardar et al., 2007]

Microstructure Changes during Service

Complex Temperature and Loading Profiles

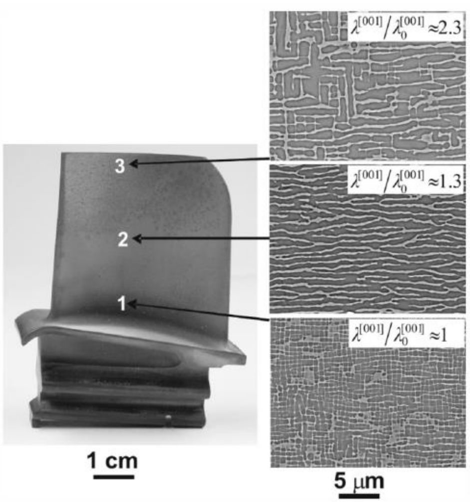

[Epishin et al., 2010]

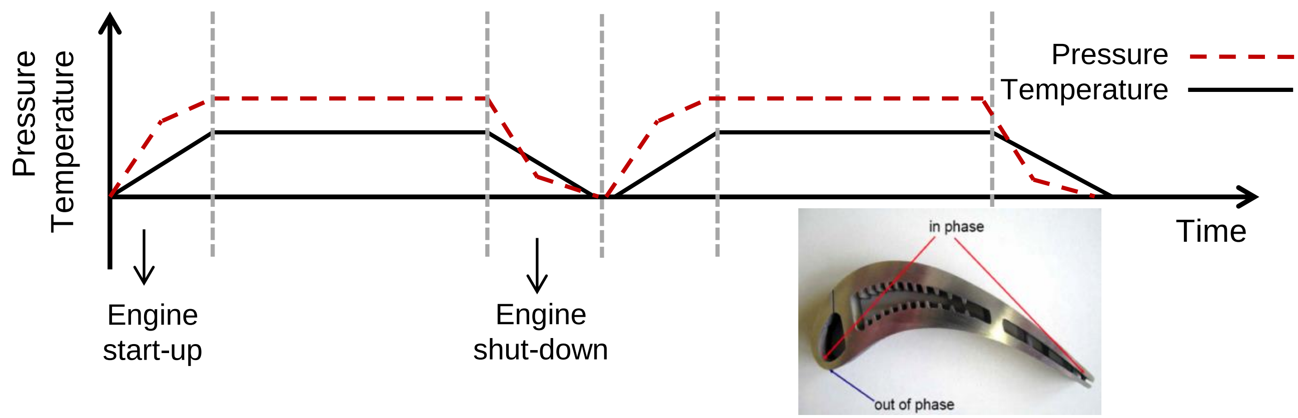

Lengths scales in the Ni-base superalloys

Atomic structure $O(10^{-10}$ m)	Channel dislocations $O(10^{-8}$ m)	Precipitate $O(10^{-7}$ m)	Groups of precipitates $O(10^{-6}$ m)	Dendrites $O(10^{-5}$ m)	Bulk $O(10^{-1}$ m)

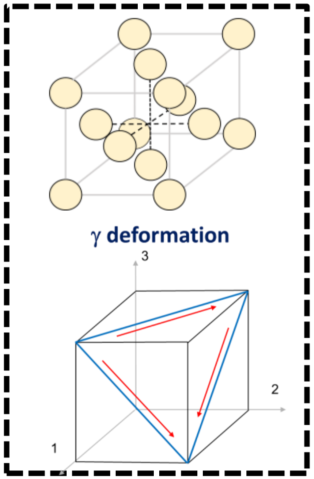

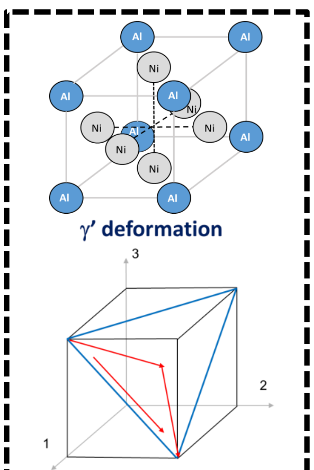

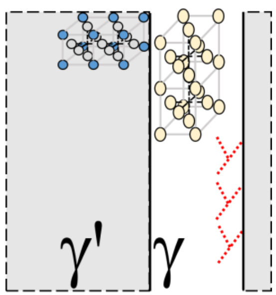

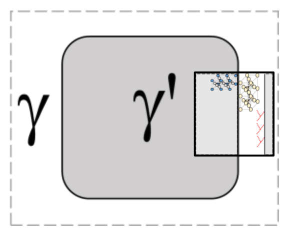

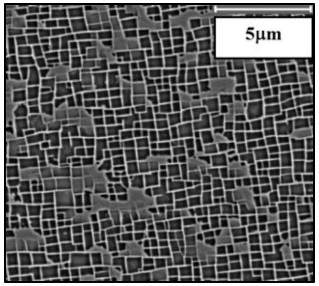

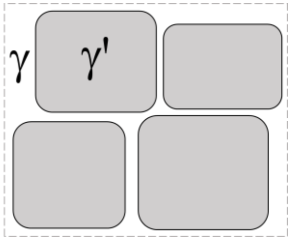

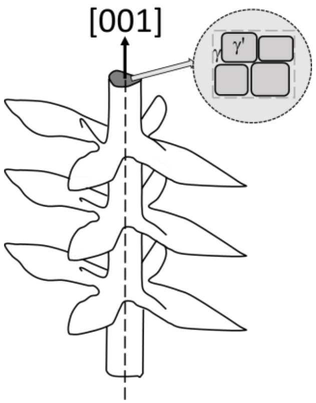

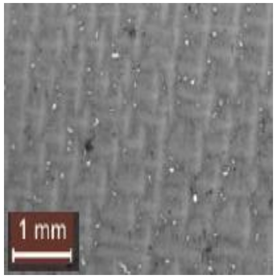

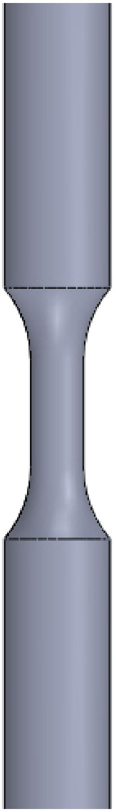

PSPP Map for Ni-base Superalloy Airfoils

The George W. Woodruff School of Mechanical Engineering
School of Materials Science and Engineering

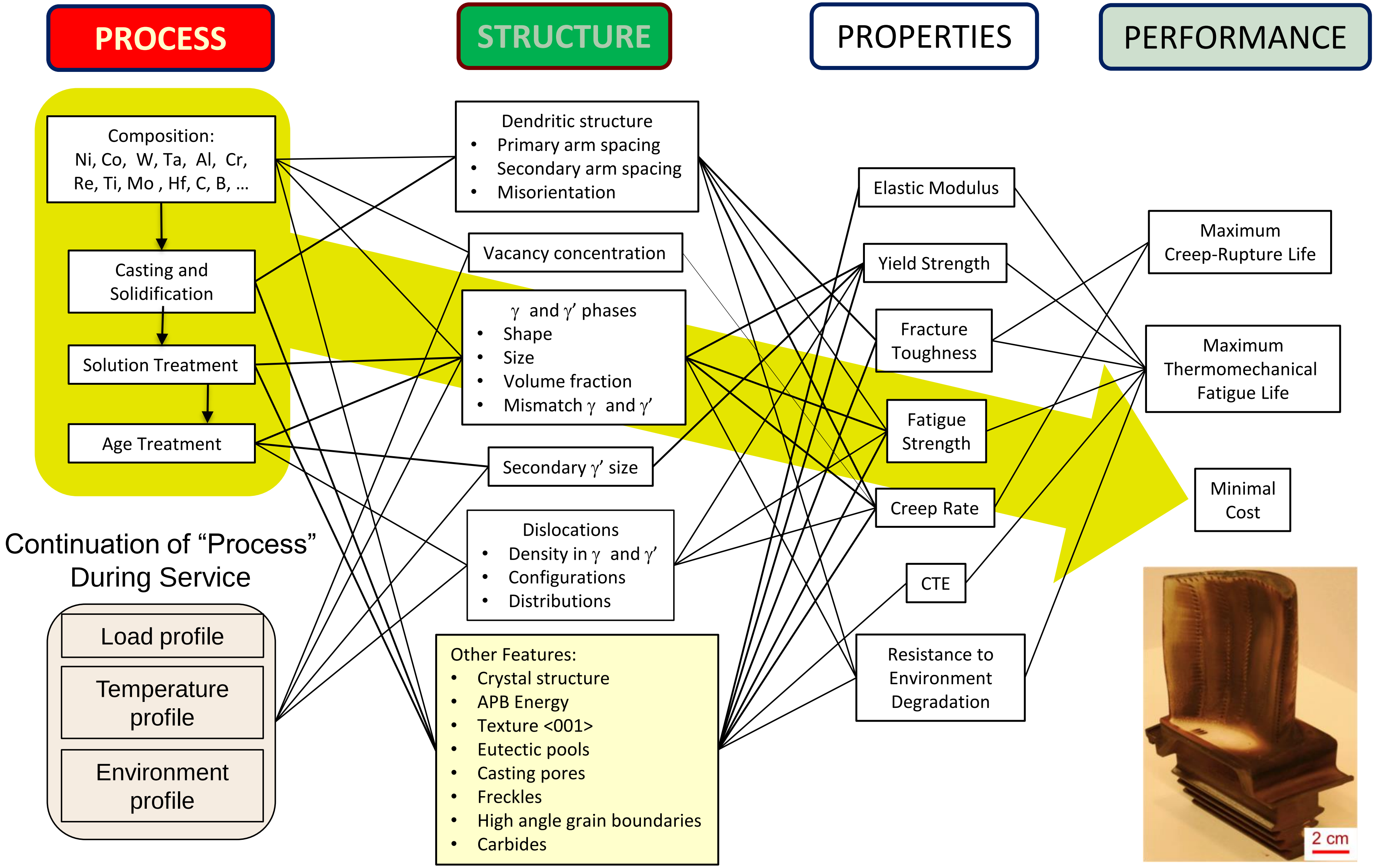

Influence of Service Conditions on Microstructure, Properties, & Performance

PROCESS

Composition:
Ni, Co, W, Ta, Al, Cr, Re, Ti, Mo, Hf, C, B, …

Casting and Solidification

Solution Treatment

Age Treatment

Continuation of "Process" During Service

- Load profile
- Temperature profile
- Environment profile

STRUCTURE

Dendritic structure
- Primary arm spacing
- Secondary arm spacing
- Misorientation

Vacancy concentration

γ and γ' phases
- Shape
- Size
- Volume fraction
- Mismatch γ and γ'

Secondary γ' size

Dislocations
- Density in γ and γ'
- Configurations
- Distributions

Other Features:
- Crystal structure
- APB Energy
- Texture <001>
- Eutectic pools
- Casting pores
- Freckles
- High angle grain boundaries
- Carbides

PROPERTIES

Elastic Modulus

Yield Strength

Fracture Toughness

Fatigue Strength

Creep Rate

CTE

Resistance to Environment Degradation

PERFORMANCE

Maximum Creep-Rupture Life

Maximum Thermomechanical Fatigue Life

Minimal Cost

Role of Chemical Composition

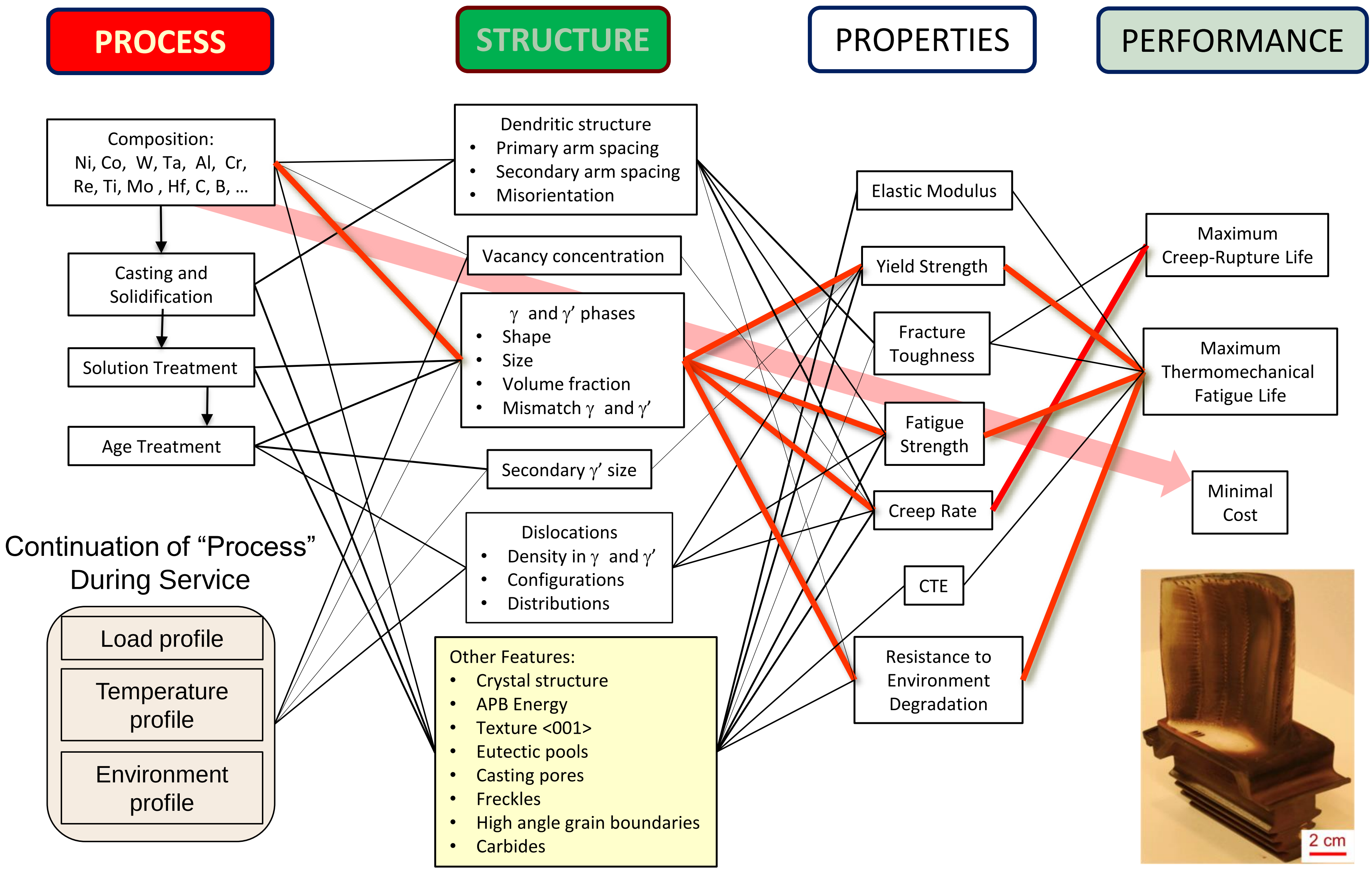

Single Crystal Alloy being Investigated for IGT Applications

CMSX-8: 1.5% Re "alternative 2nd gen alloy" replacing 3.0% Re containing alloys (e.g., CMSX-4, PWA1484)

Alloy	Cr	Co	Mo	W	Al	Ti	Ta	Re	Hf	C	B	Zr	Ni
Mar-M247LC-DS	8.4	10.0	0.7	10.0	5.5	1.0	3.0	-	1.5	0.07	0.015	0.05	Bal
CM247LC-DS	8.1	9.2	0.5	9.5	5.6	0.7	3.2	-	1.4	0.07	0.015	0.01	Bal
CMSX-4	6.5	9.0	0.6	6.0	5.6	1.0	6.5	3.0	0.1	-	-	-	Bal
SC16	16	0.17	3.0	0.16	3.5	3.5	3.5	-	-	-	-	-	Bal
PWA1484	5.0	10.0	2.0	6.0	5.6	-	9.0	3.0	0.1	-	-	-	Bal
CMSX-8	5.4	10.0	0.6	8.0	5.7	0.7	8.0	1.5	0.2	-	-	-	Bal

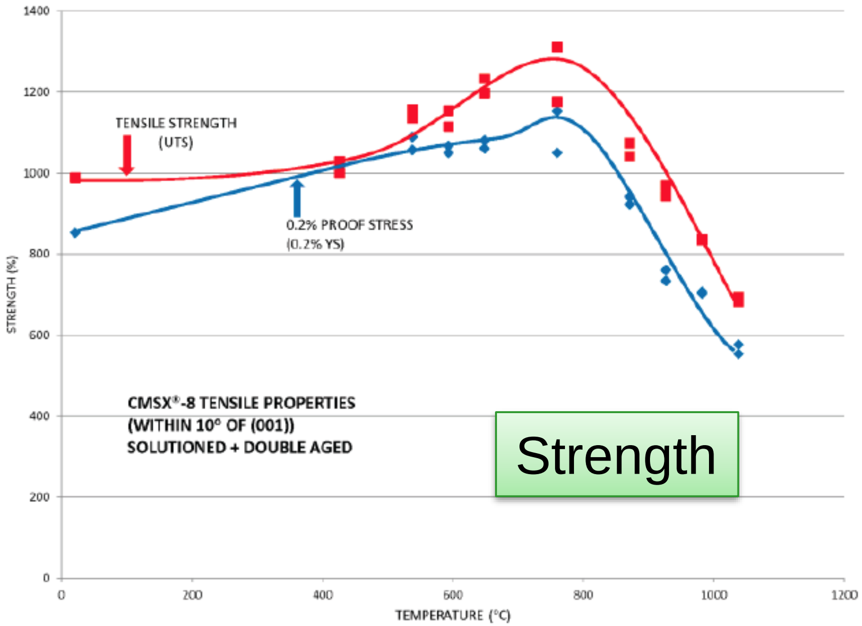

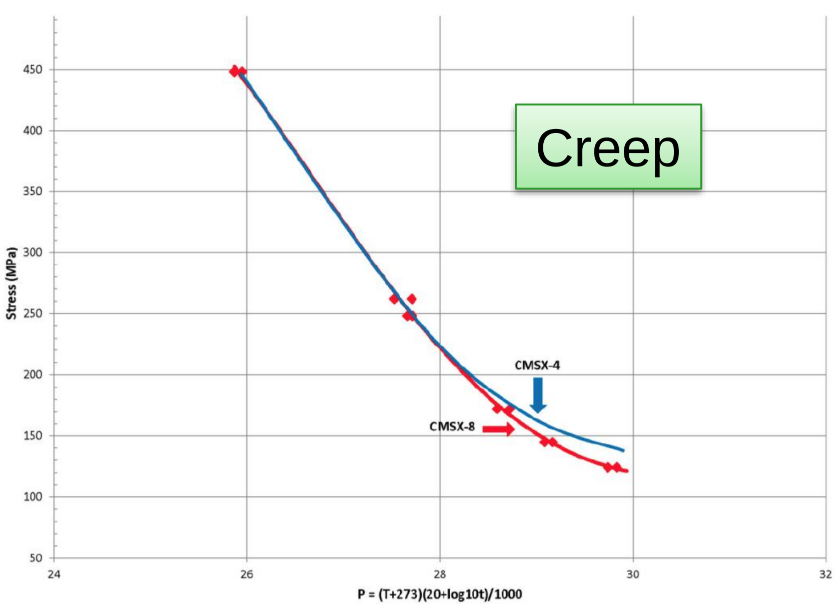

[Wahl and Harris, 2012]

Influence of Temperature, Loading Direction and Crystal Orientation on Modulus and Strength

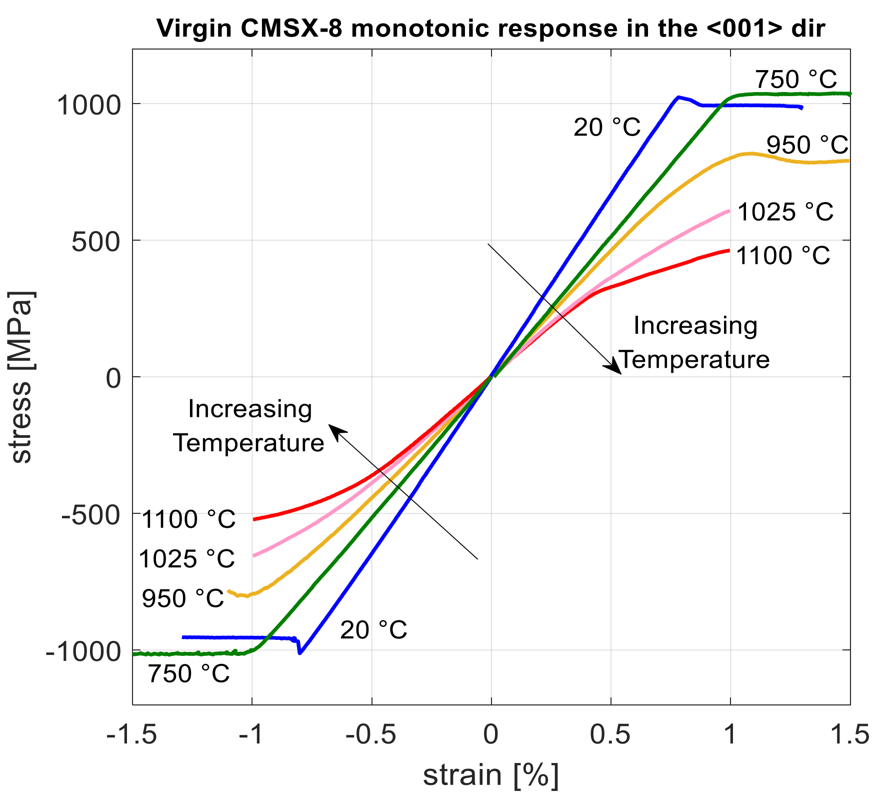

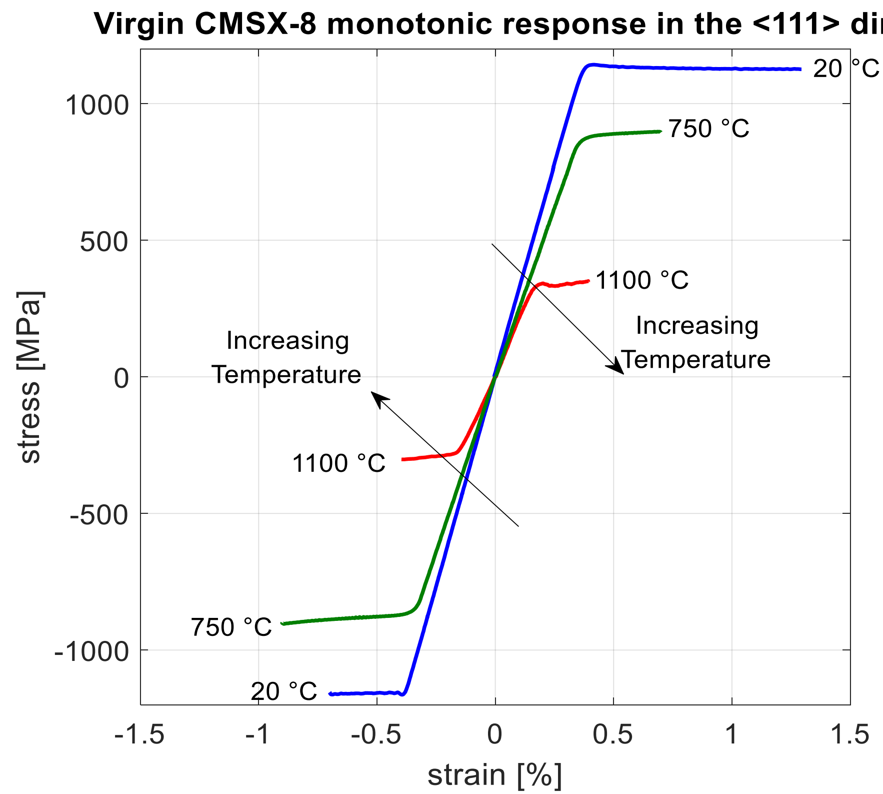

Primary Objectives of UTSR Project

- Creep-fatigue interaction experiments on CMSX-8
- Influence of aging on microstructure and creep-fatigue interactions
- Microstructure-sensitive, temperature-dependent crystal viscoplasticity to capture the creep and cyclic deformation response

Georgia Institute of Technology

Creep-Fatigue Interaction Experiments

The George W. Woodruff School of Mechanical Engineering　　School of Materials Science and Engineering

Experimentally establish the creep-fatigue interactions in a single-crystal Ni-base superalloy that is being targeted for use in industrial gas turbines (CMSX-8)

- Characterize creep-fatigue interactions on CMSX-8
  - Creep-fatigue
  - Thermomechanical fatigue
  - Creep (either tension or compression) followed by fatigue
  - Fatigue followed by creep
- Characterize the influence of aging on microstructure and creep-fatigue interactions

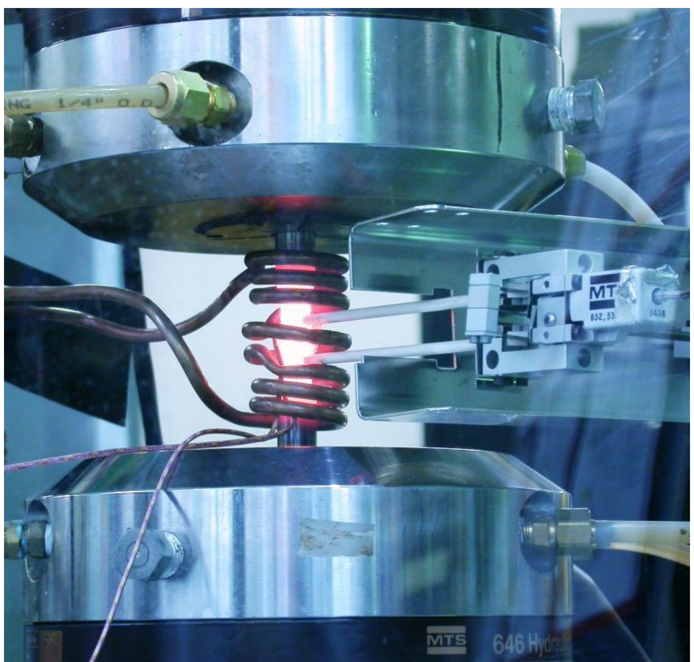

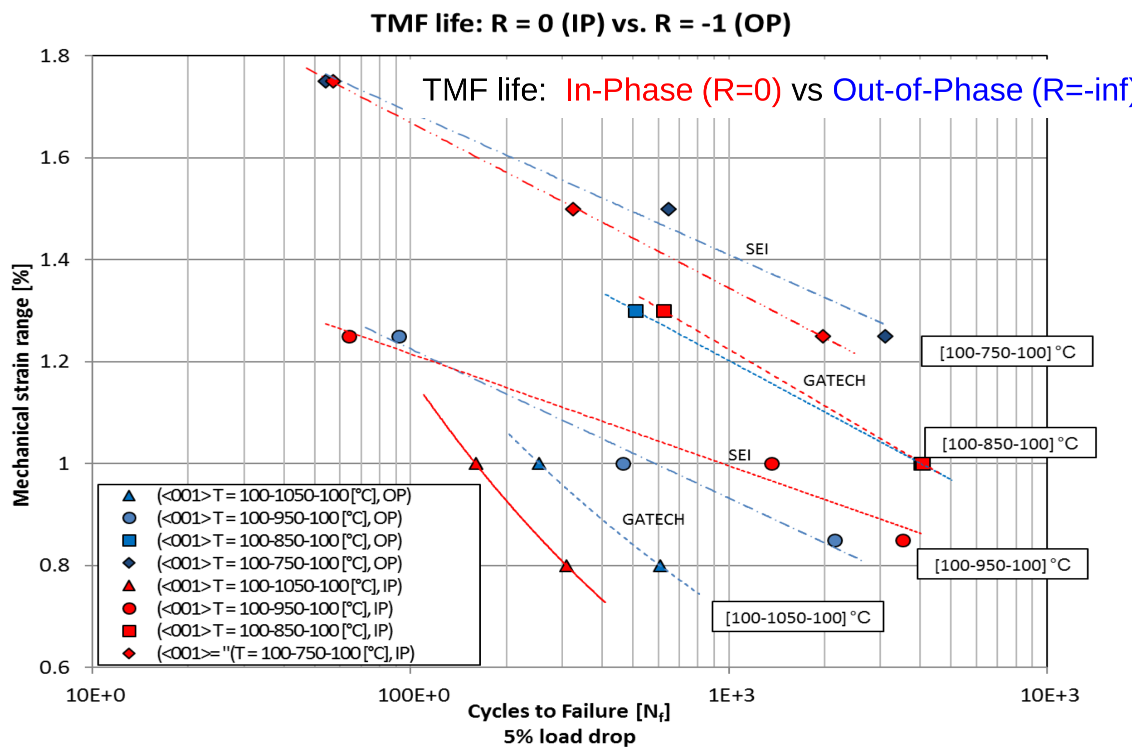

Conventional Creep-Fatigue (baseline)

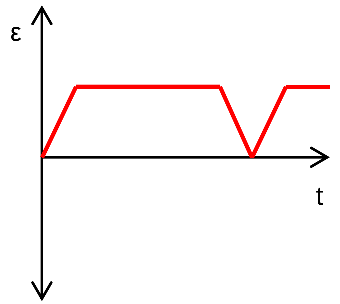

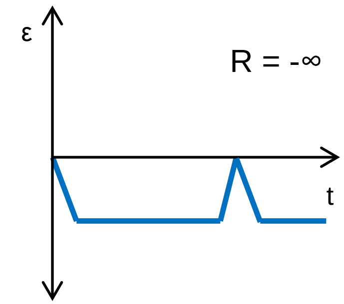

Effect of hold on LCF life: R = 0

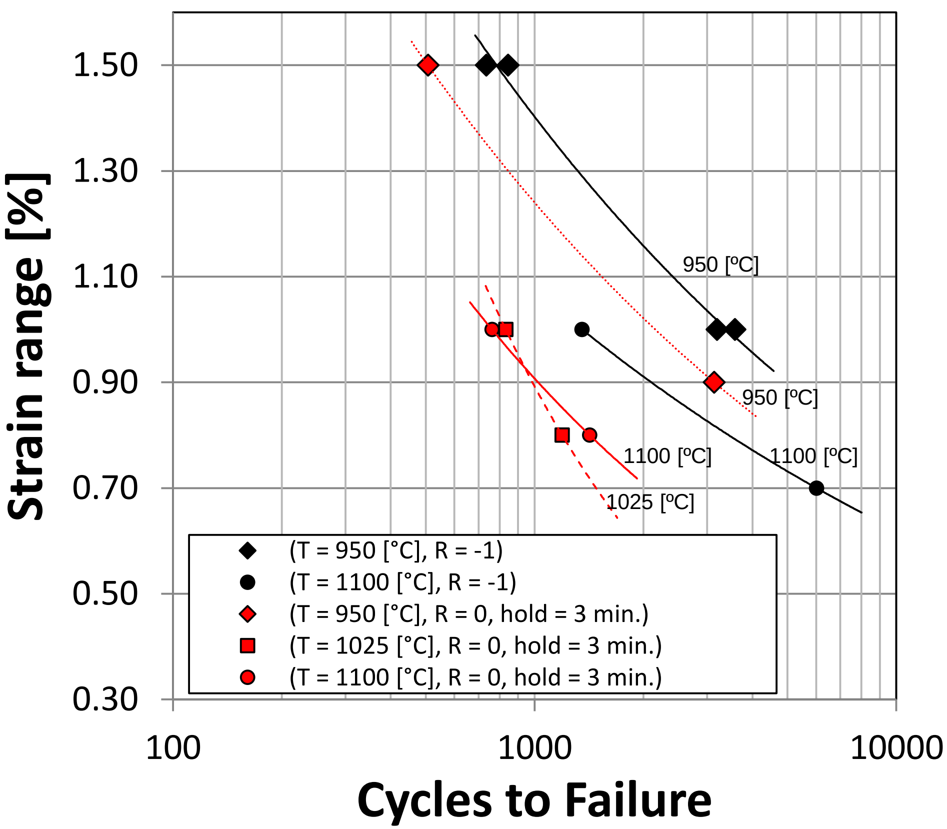

Effect of hold on LCF life: R = -∞

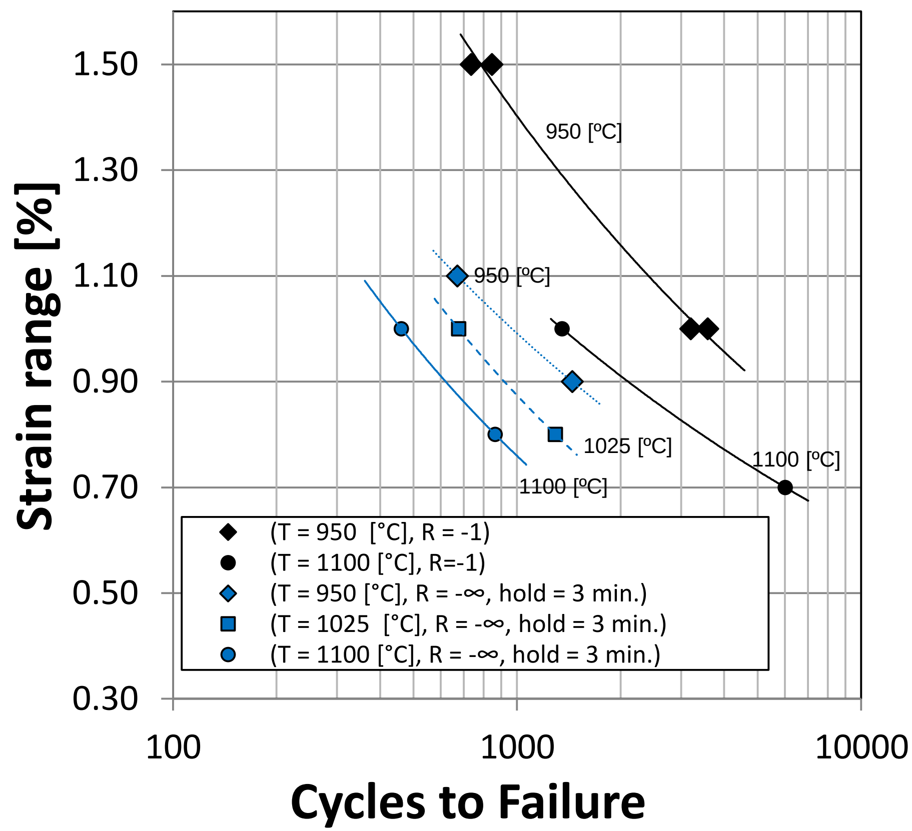

Conventional Creep-Fatigue (baseline)

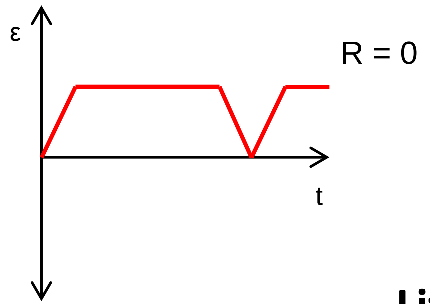

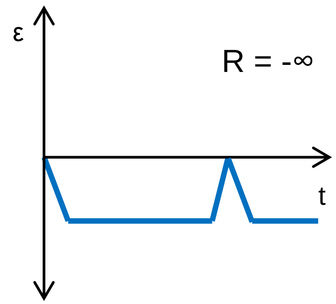

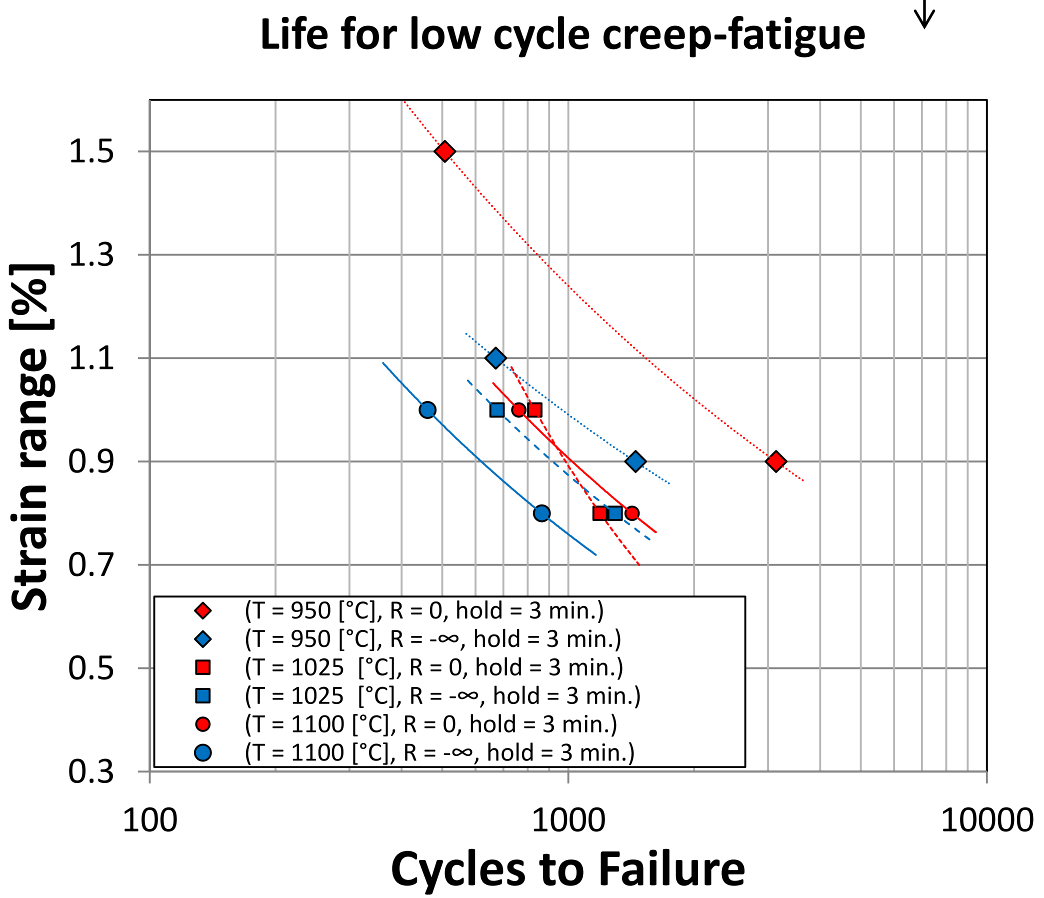

Half-life at 1100 ºC

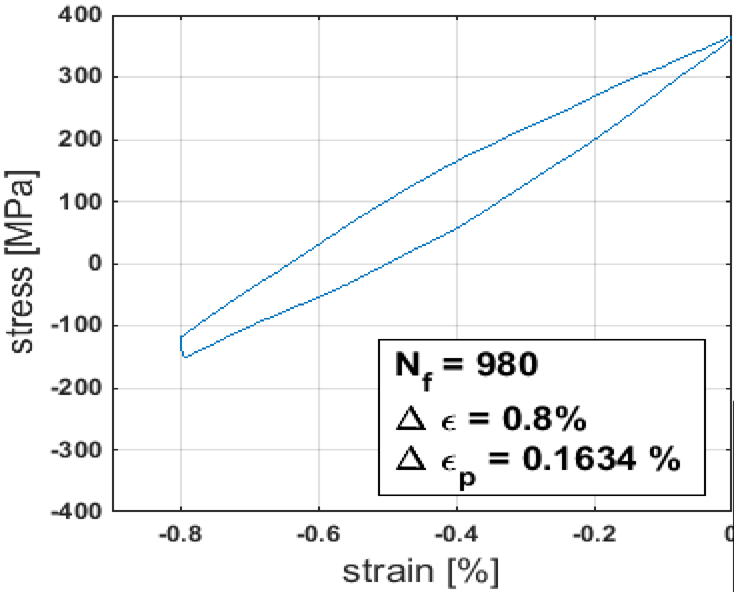

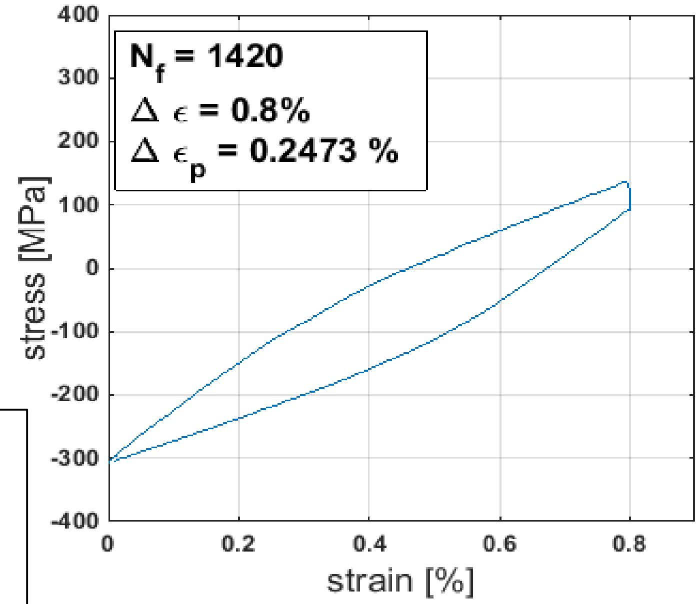

$\Delta\varepsilon$ = 0.8 [%]

Plastic strain range alone does not explain life data at high temperatures. A Coffin-Manson relations would not be sufficient

$\Delta\varepsilon$ = 1.0 [%]

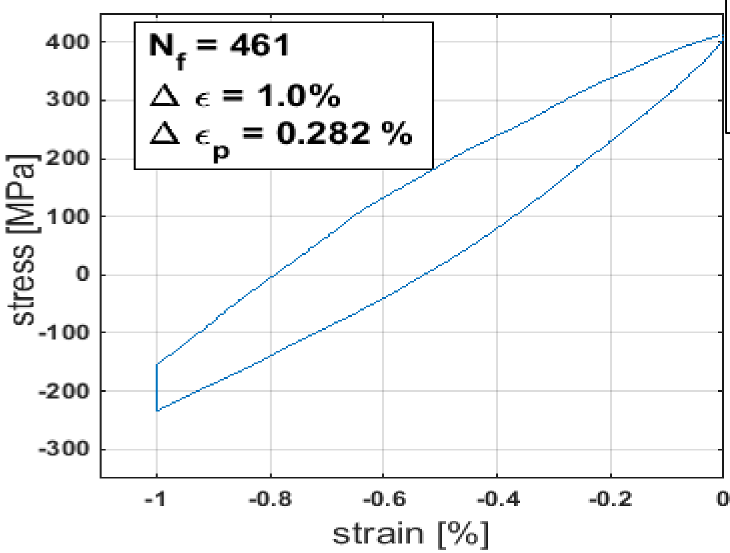

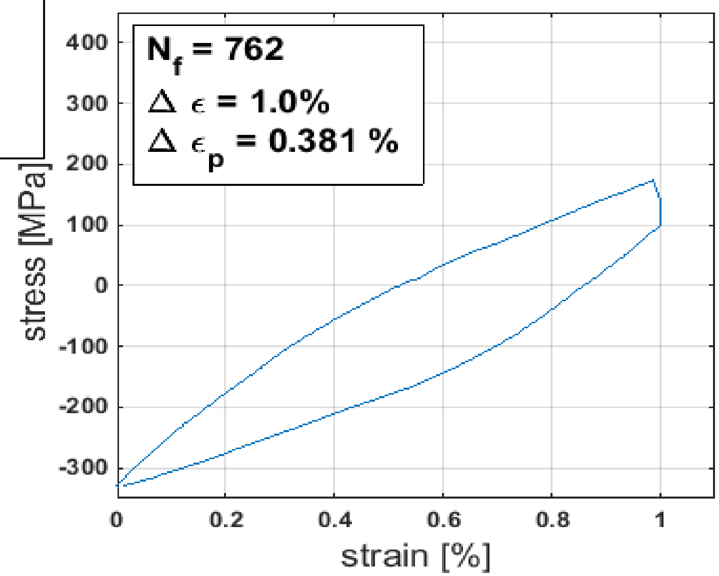

Crack Characteristics

R = 0, T = 1100ºC, $\Delta\varepsilon$ = 0.8%
N_f = 1420

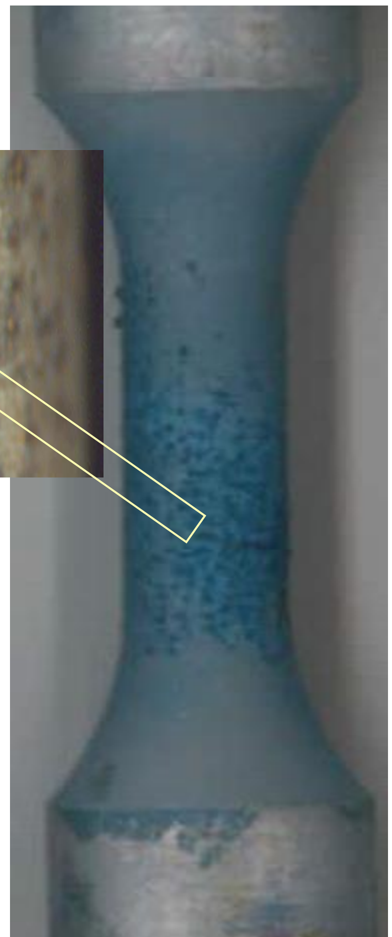

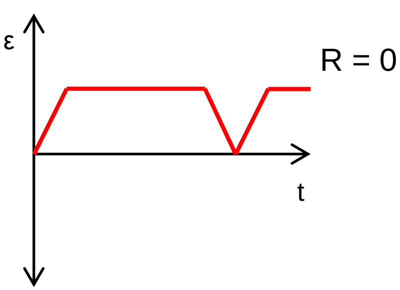

R = -∞, T = 1100ºC, $\Delta\varepsilon$ = 0.8%
N_f = 980

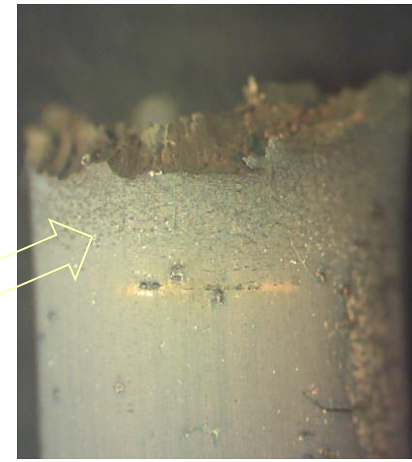

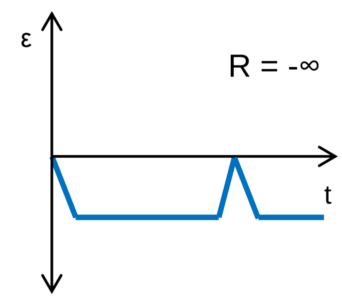

Fatigue Lifetime Models - I

Ostergren Model

- Energy-based life prediction model based on the net hysteretic energy.
- Accounts for the mean stress and cycle time (frequency) effect.
- The accuracy of prediction relies on precision of inelastic strain measurement.

$$\sigma_T \, \Delta\varepsilon_P \; N_f^{\beta} \; \upsilon^{\beta(k-I)} = C$$

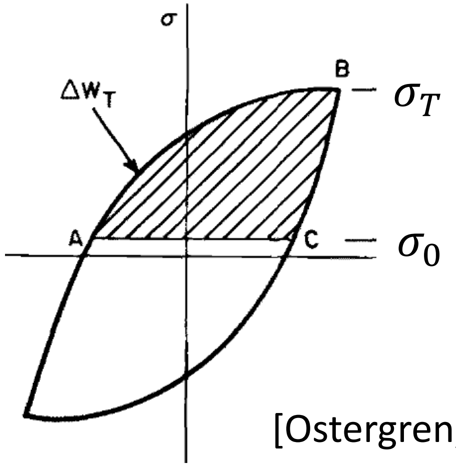

[Ostergren, 1976]

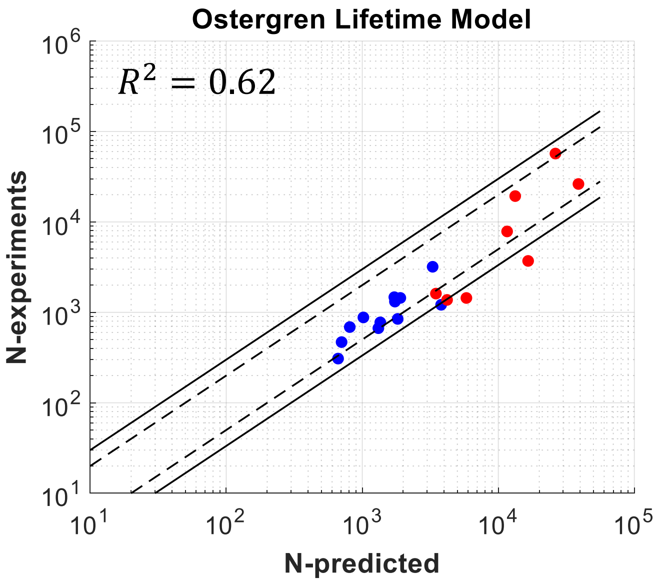

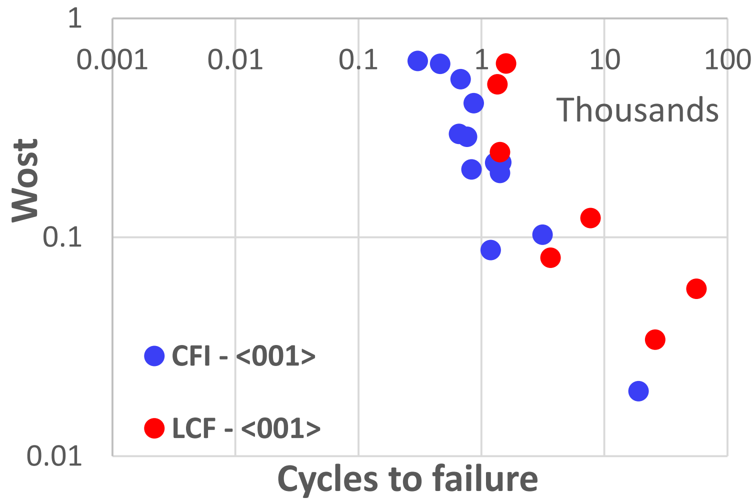

Fatigue Lifetime Models - II

Zamrik and Renauld Model

- Introducing hold-time and elevated temperature function to account for creep effect and exponentially increasing creep/or environmental damage with increasing temperature, respectively.
- Substituting inelastic strain with maximum tensile strain range.

$$N = A\left[\underbrace{\left(\frac{\varepsilon_{ten}}{\varepsilon_f}\right)\left(\frac{\sigma_{max}}{\sigma_u}\right)}_{W_{zam}}\right]^B \left(1+\frac{t_h}{t_c}\right)^C exp\left(\frac{-Q}{R(T_{max}-T_0)}\right)$$

σ_{max} : maximum tensile stress in mid-life hysteresis loop

ε_{ten} : tensile strain range in mid-life hysteresis loop for which the stress is tensile

σ_u : ultimate strength measured under monotonic tensile loading

ε_f : elongation to failure measured under monotonic tensile loading

t_h: length of compressive hold-time

t_c: length of total time including hold-time

Q: activation energy for high temperature damage

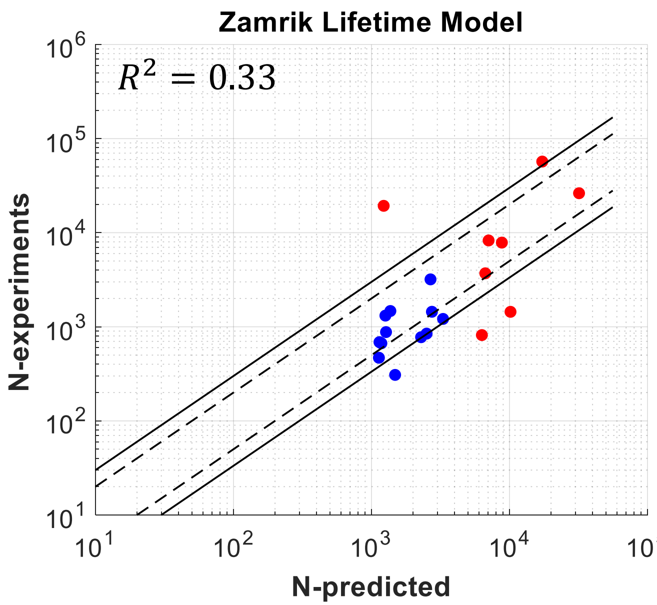

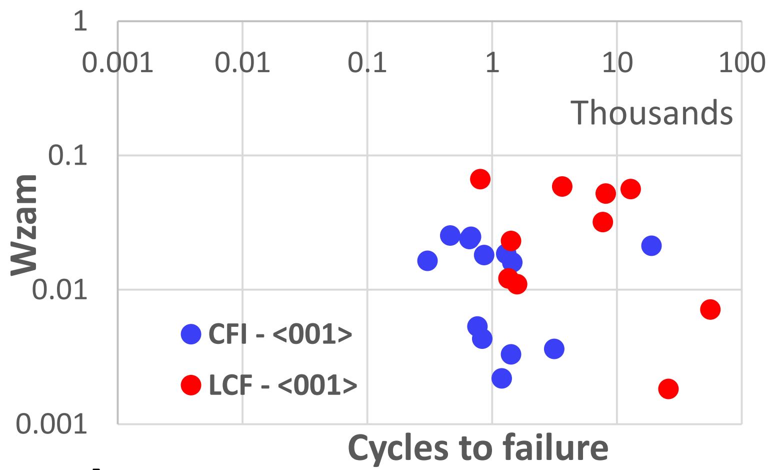

[Zamrik and Renauld, 2000]

Fatigue Lifetime Models - III

Kulawinski et al. Model

- The model is based on Zamrik model and the energy density term includes:

  - Zamrik damage parameter
  - Inelastic strain range
  - Stress range
  - Arrhenius term

$$N_f = A\left[\underbrace{\Delta\sigma_{eq}.\Delta\varepsilon_{eq}^{in}.W_{zam}}_{W_{Kul}}.\,exp\left(\frac{-Q}{RT}\right)\right]^B$$

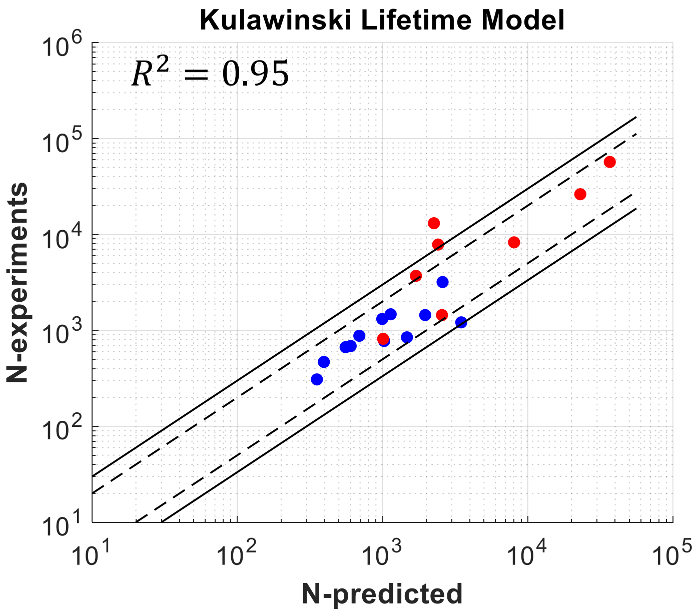

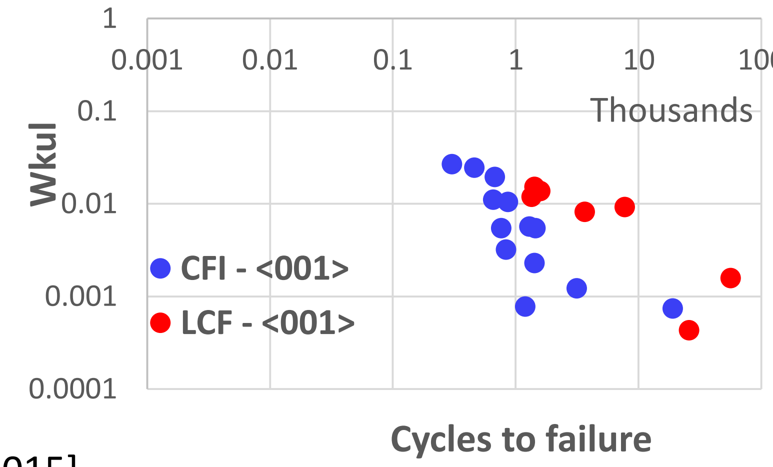

- The goodness of fit plot shows majority of life predictions using Kulawinski model lie within the scatter band of factor two.

- 95% of the variance of the low cycle fatigue (LCF) and creep-fatigue (CFI) life data is captured by this lifetime model.

[Kulawinski et al., 2015]

Primary Objectives of UTSR Project

- Creep-fatigue interaction experiments on CMSX-8
- Influence of aging on microstructure and creep-fatigue interactions
- Microstructure-sensitive, temperature-dependent crystal viscoplasticity to capture the creep and cyclic deformation response

Microstructure Evolution in Blades

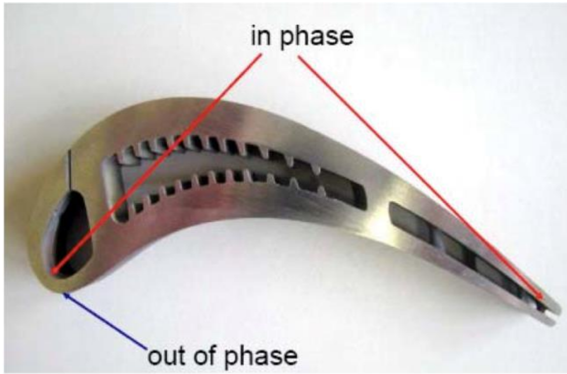

Distance from Root

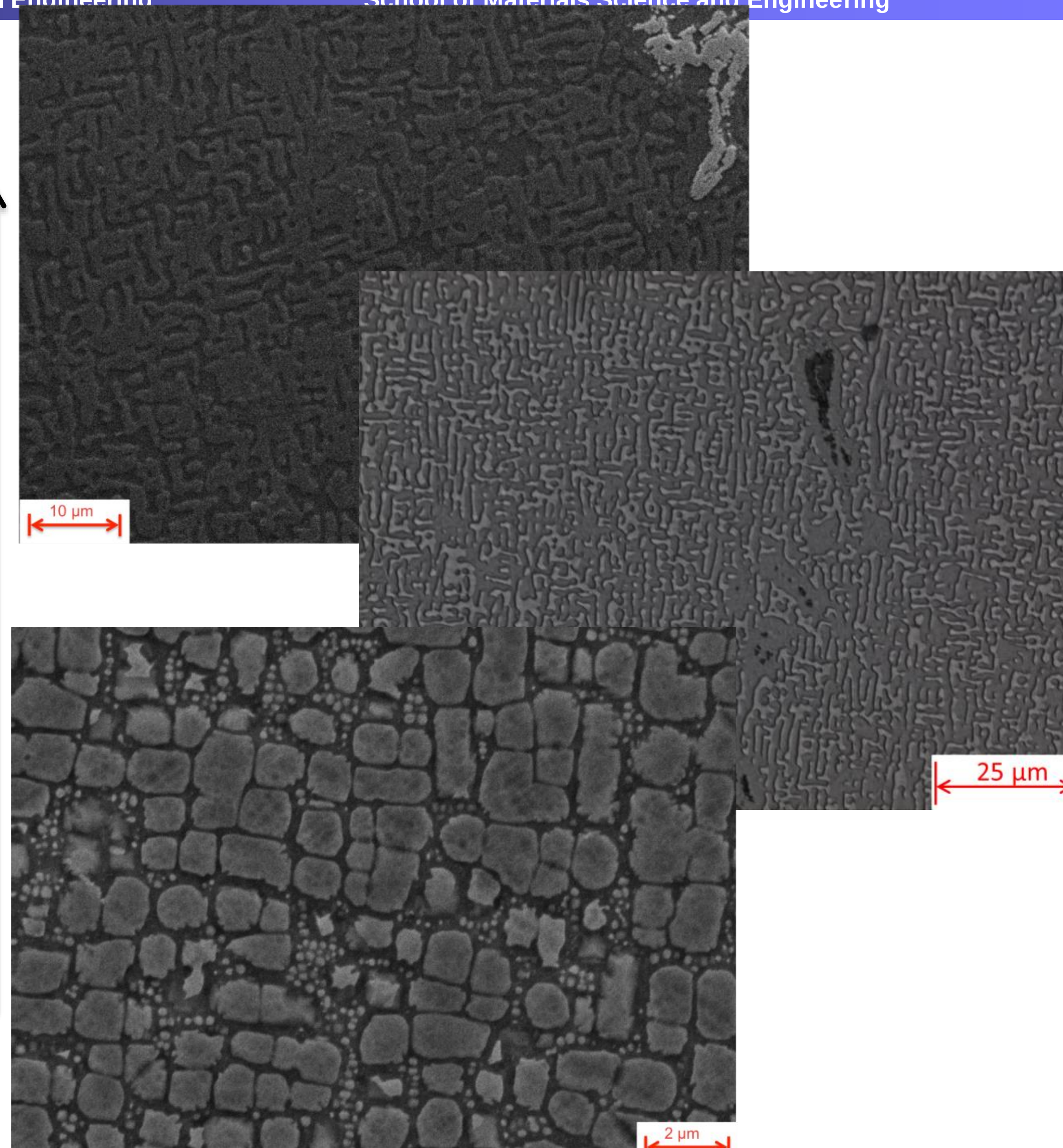

Microstructures Generated by Additive Manufacturing

CMSX-4 via Scanning Laser Epitaxy (SLE)

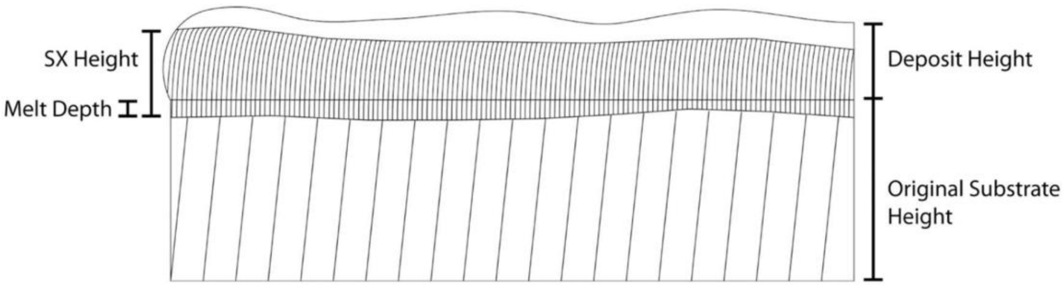

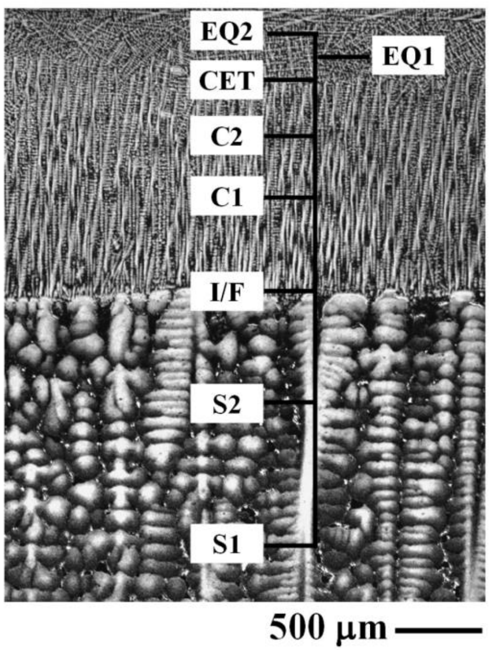

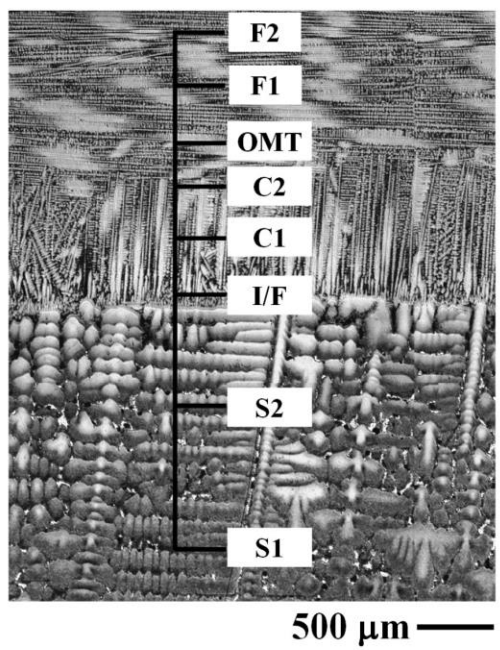

As-built

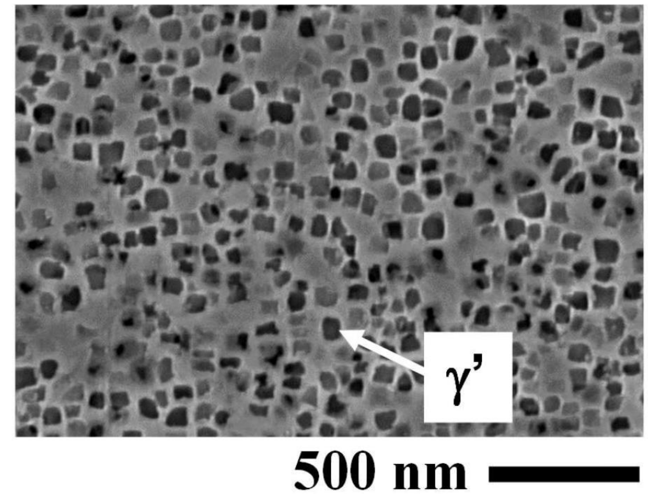

After Heat Treatment

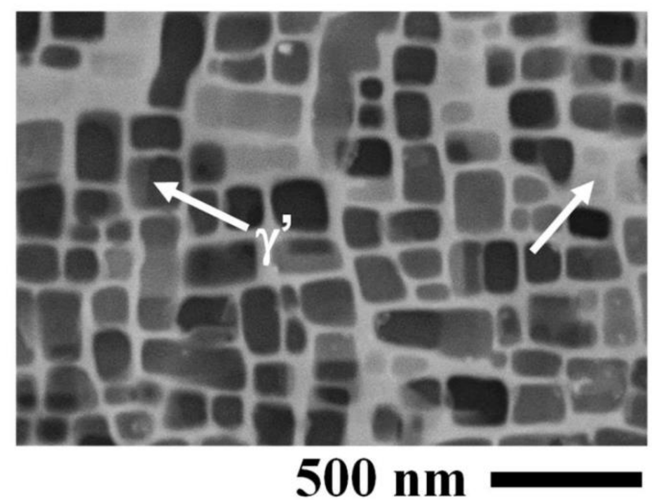

[Basak and Das (Georgia Tech), 2017]

Rafting and Coarsening of γ’

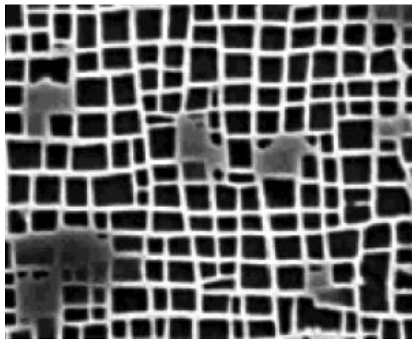

Tension

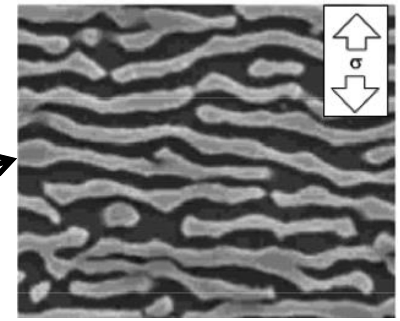

N-raft

Compression

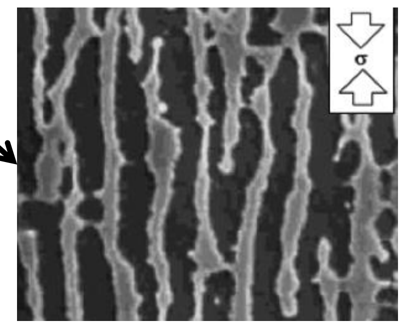

P-raft

$$\delta = \frac{2(a_{\gamma'} - a_{\gamma})}{a_{\gamma'} + a_{\gamma}}$$

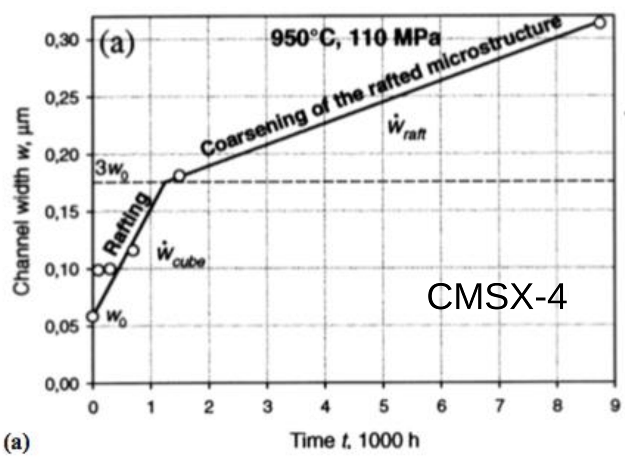

(a)

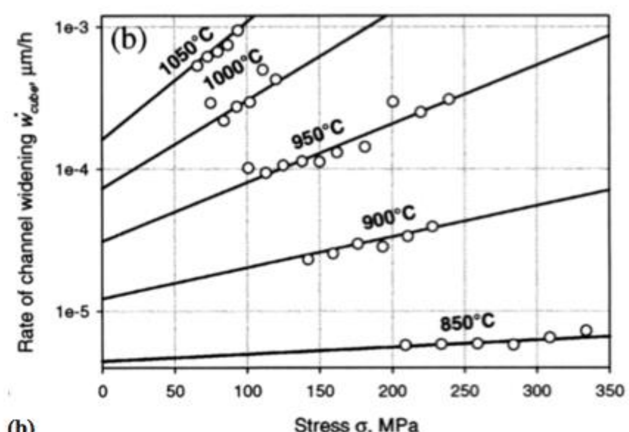

(b)

[Epishin et al., 2008]

High-Throughput Stress-assisted Aging

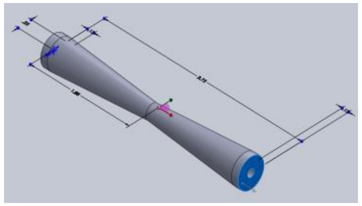

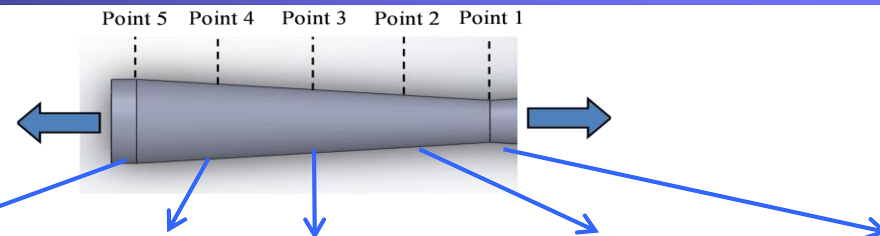

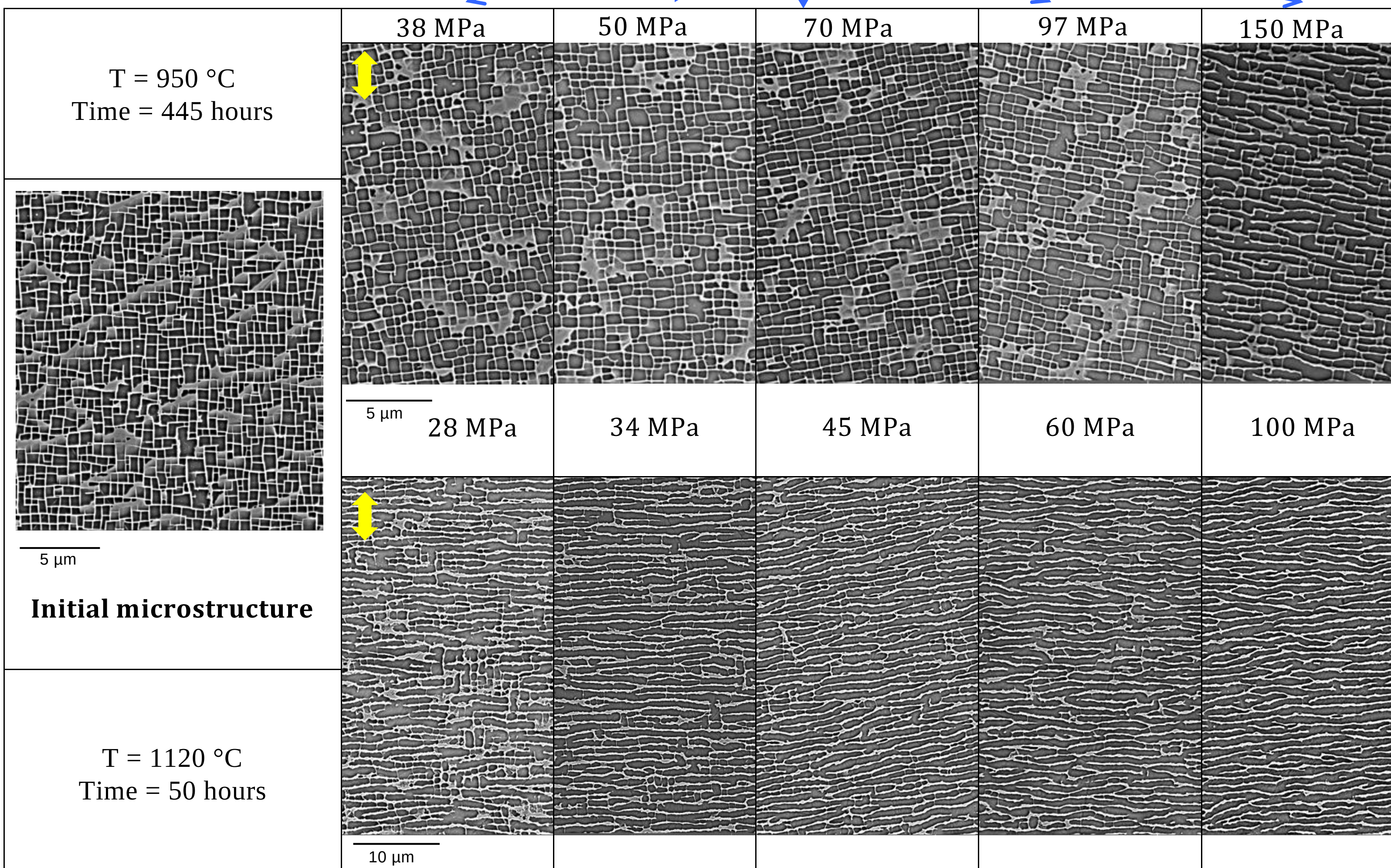

Aged Microstructure under Compressive Stress

Compression Creep Frame

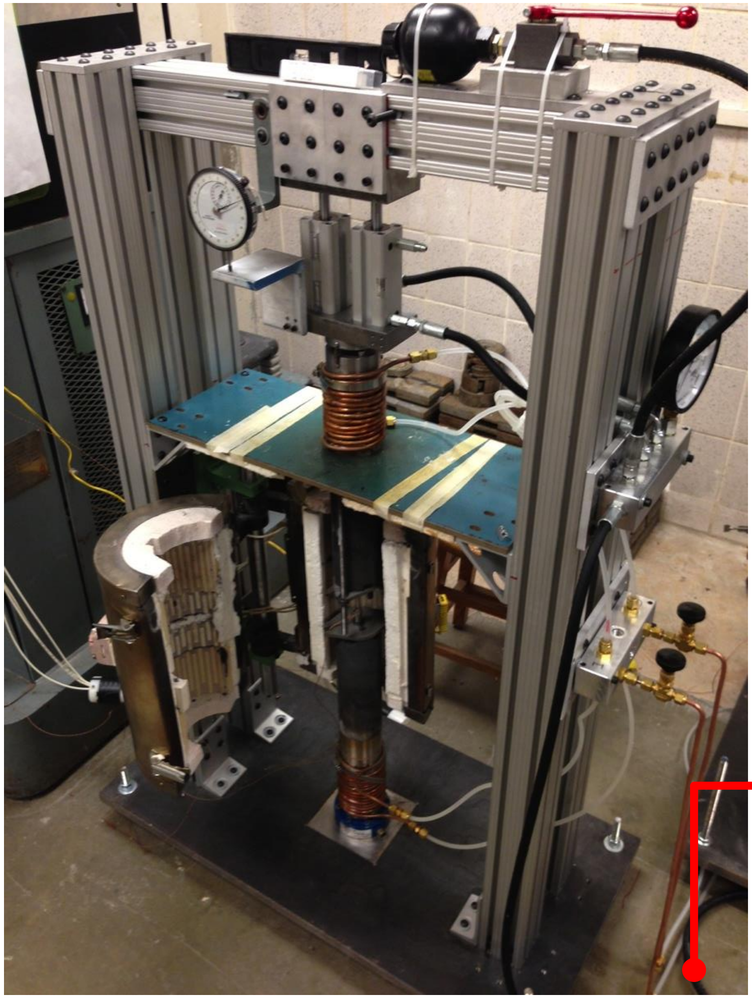

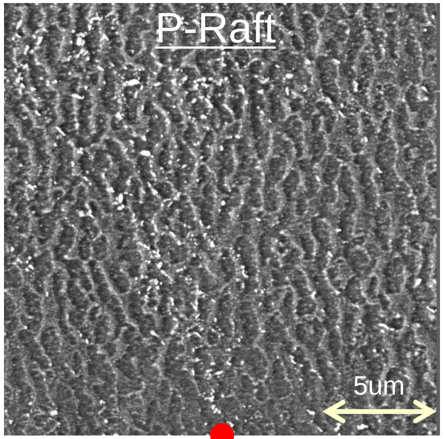

Ceramic Compression Creep Extensometer

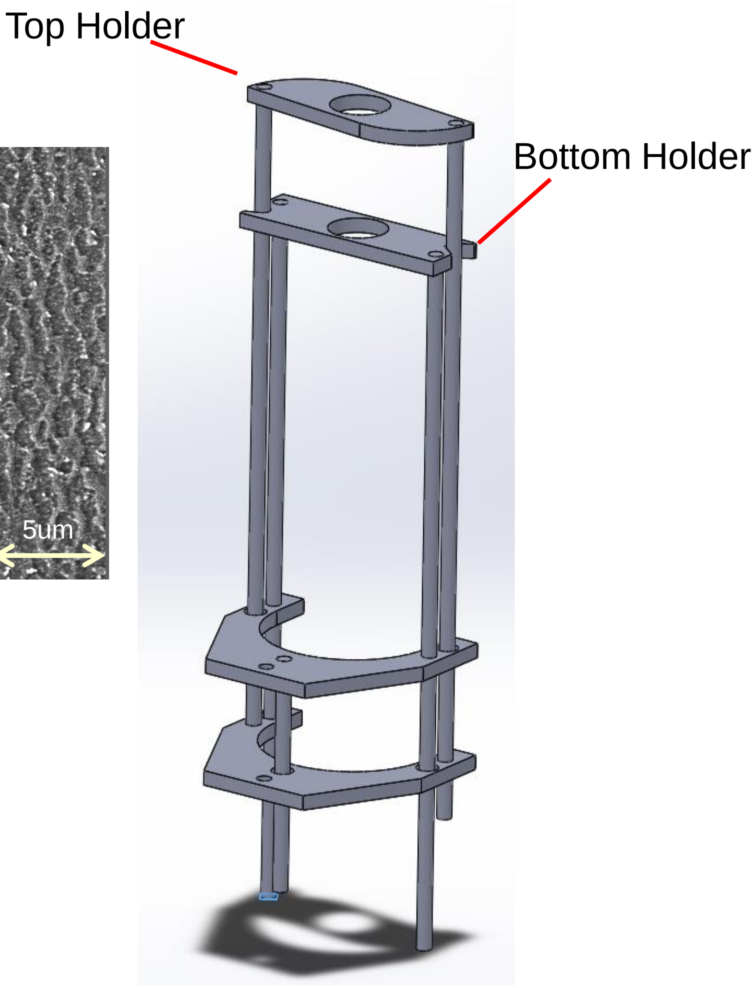

Aging Behavior of CMSX-8

Physical aging models

Directional coarsening (Rafting)

$$\dot{w}(T,\sigma) = A.exp\left[-\frac{Q - U(T).\sigma}{RT}\right]$$

$$U(T) = U_T(T - T_0)^n$$

[Epishin et al., 2008]

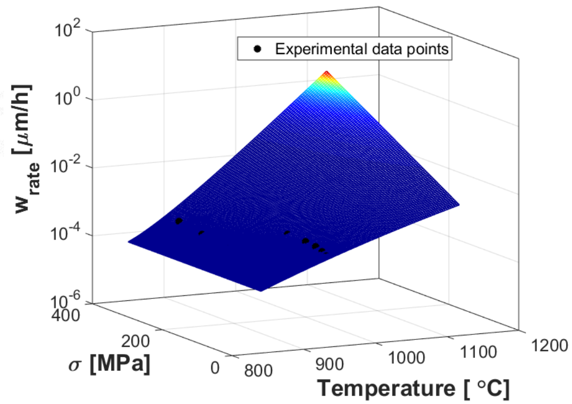

Isotropic Coarsening

Lifshitz-Slyozov-Wagner (LSW) model:

$$(r)^3 - (r_0)^3 = Kt$$

$$K = K_0\, exp\left(-\frac{Q_{coar}}{RT}\right)$$

$$Q_{coar}\,(CMSX-8) = 269.4\ kJ/mol$$

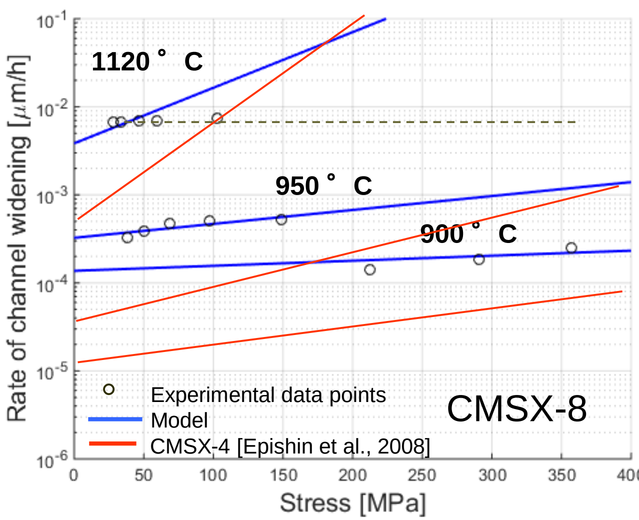

High-throughput experimental technique

Stress gradient in longitudinal direction resulting in morphology evolution gradient

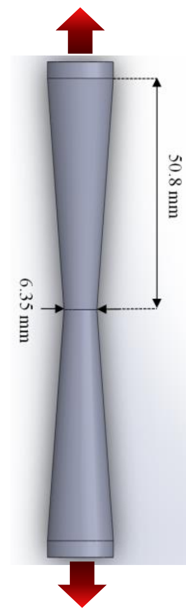

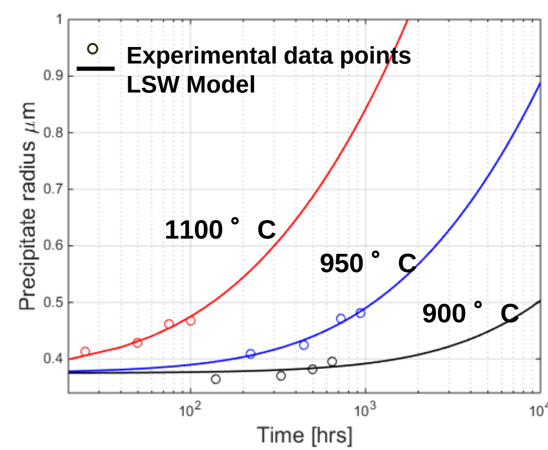

[Gorgannejad, Estrada Rodos, and Neu, *Materials at High Temperature*, 2016]

Influence of Variation in Composition

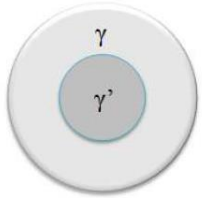

Thermo-Calc
DICTRA
Databases: TCNi5 / MOBNi2

Composition sensitive diffusivity parameter

Aging behavior

Temperature-dependent constitutive models

LSW model

$$r^3 - r_o^3 = K\left(t - t_o\right)$$

$$K = \frac{64 D_{eff} C_\infty \sigma \Omega^2}{9RT}$$

$$D_{eff} = D_{0,eff}\left(-\frac{Q_{eff}}{RT}\right)$$

Coarsening effective diffusivity

$$\dot{g}^a = \dot{g}_0 Q(T) \left\langle \frac{t_u^a}{D^a} \right\rangle^n \exp\left\{ B_0 \left\langle \frac{t_u^a}{D^a} \right\rangle^{n+1} \right\} \mathrm{sgn}(t^a - c^a)$$

$$Q(T) = \exp\left(-\frac{Q_0}{RT}\right)$$

Diffusivity parameter

Composition segregation
Thermo-Calc

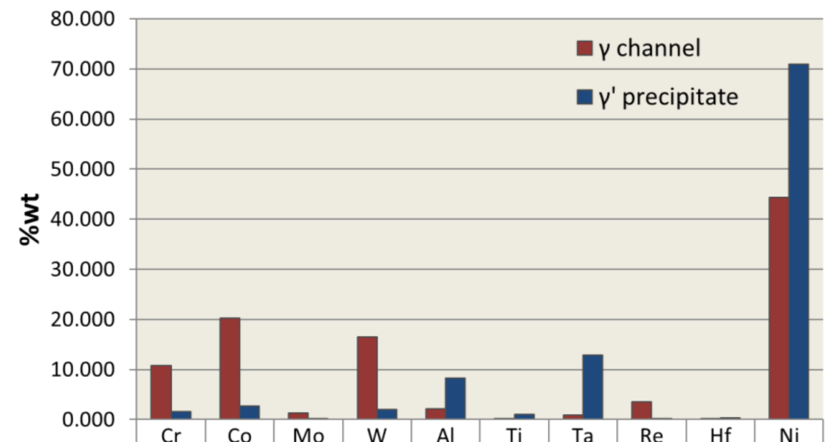

	Cr	Co	Mo	W	Al	Ti	Ta	Re	Hf	Ni
γ channel	10.82	20.31	1.260	16.52	2.080	0.170	0.940	3.520	0.012	44.38
γ' precipitate	1.610	2.690	0.130	2.030	8.230	1.070	12.93	0.110	0.330	70.87

Influence of Re Content on Diffusivity

- Effective diffusivity of system is equivalent to effective diffusivity in γ channels.
- Diffusivity of Ni-m binary systems computed from mobility databases using DICTRA from Thermo-Calc.

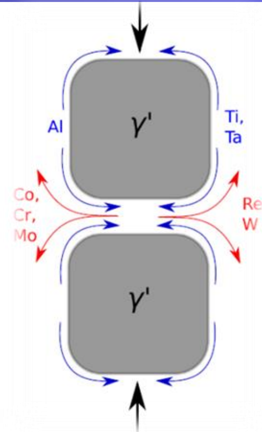

[Mushongera et al. 2015]

$$D_{eff} = D_{0,eff}\,exp\left(-\frac{Q_{eff}}{kT}\right)$$

$$Q_{eff} = \sum_m C_m Q_{Ni-m}$$

$$D_{0,eff} = \frac{1}{\sum_m \frac{C_m}{D_{0,Ni-m}}}$$

[Ai et al. 2015]

* C_m : atomic concentration of element m

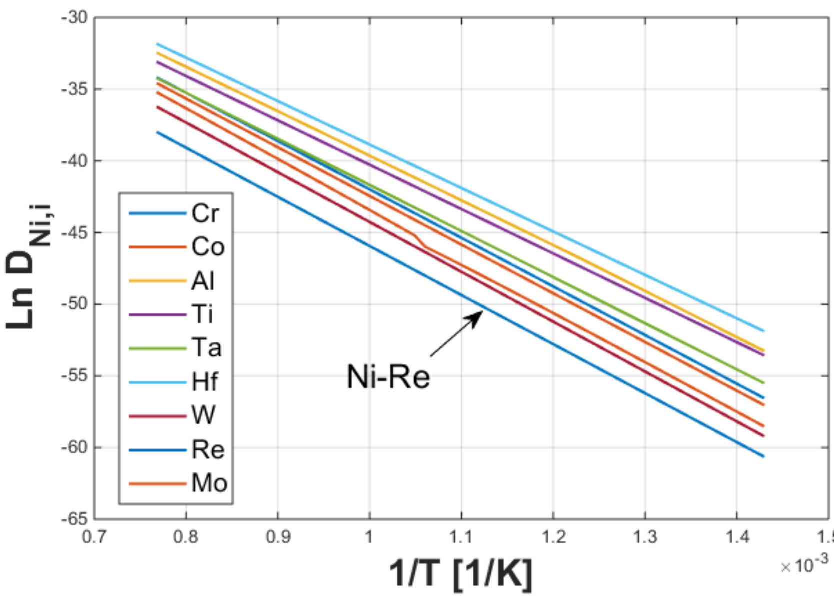

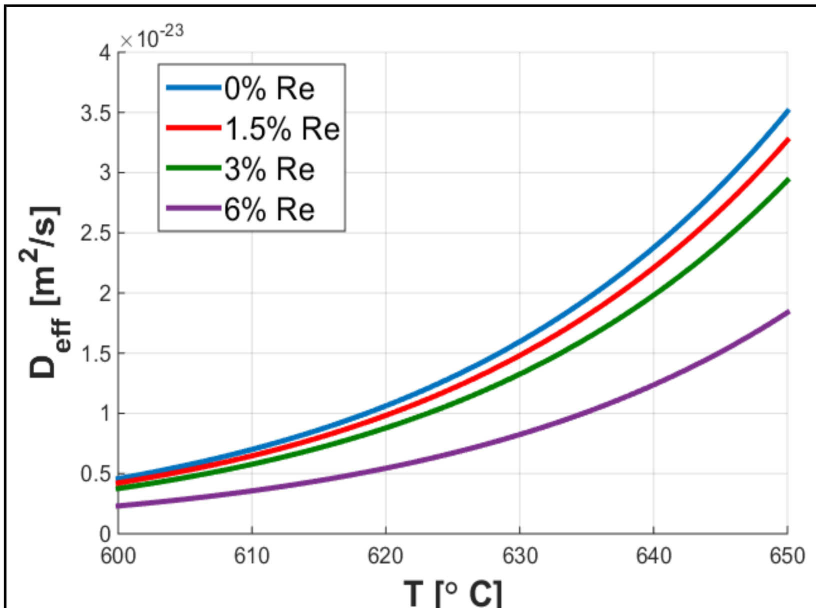

[Estrada Rodas, Gorgannejad, Neu, et al., Superalloys 2016]

Employing Data Science to Predict Aged Structure

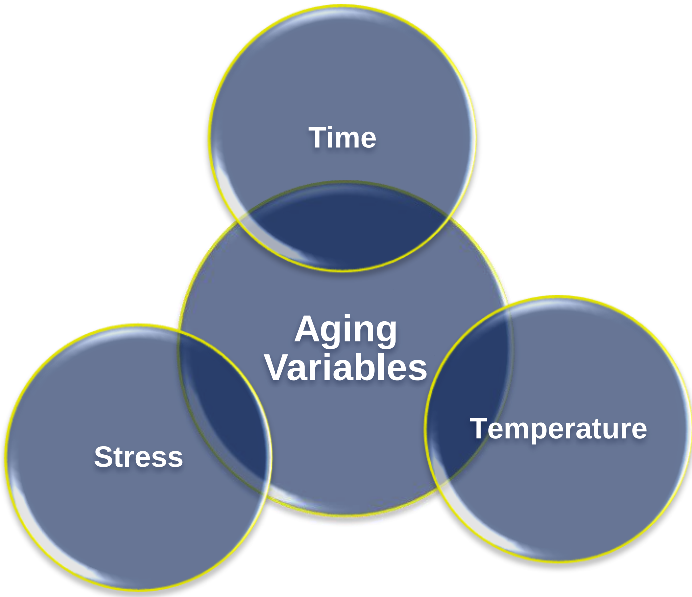

Process – Structure Relation

γ and γ´ phases

- Spatial distribution
- Volume fraction
- Size
- Morphology and shape

Experimental Database → Discretizing the Database → Quantification of Microstructure → Dimensionality Reduction → Model Construction

A database comprising of coarsened and rafted (P-type and N-type) microstructure as a result of various aging histories is generated

Tracking Microstructure Evolution

- The 2-point statisical correlation is a rigorous quantification method that describes spatial correlation and critical structural information with microstructure reconstruction capability.

- It is computed based on the probability density associated with finding an ordered pair of specific phase at the head and tail of a randomly placed vector $\boldsymbol{r}$ into the microstructure.

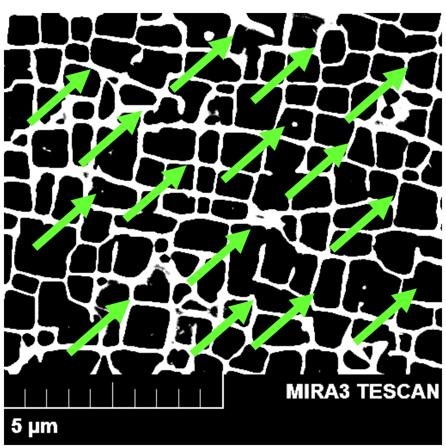

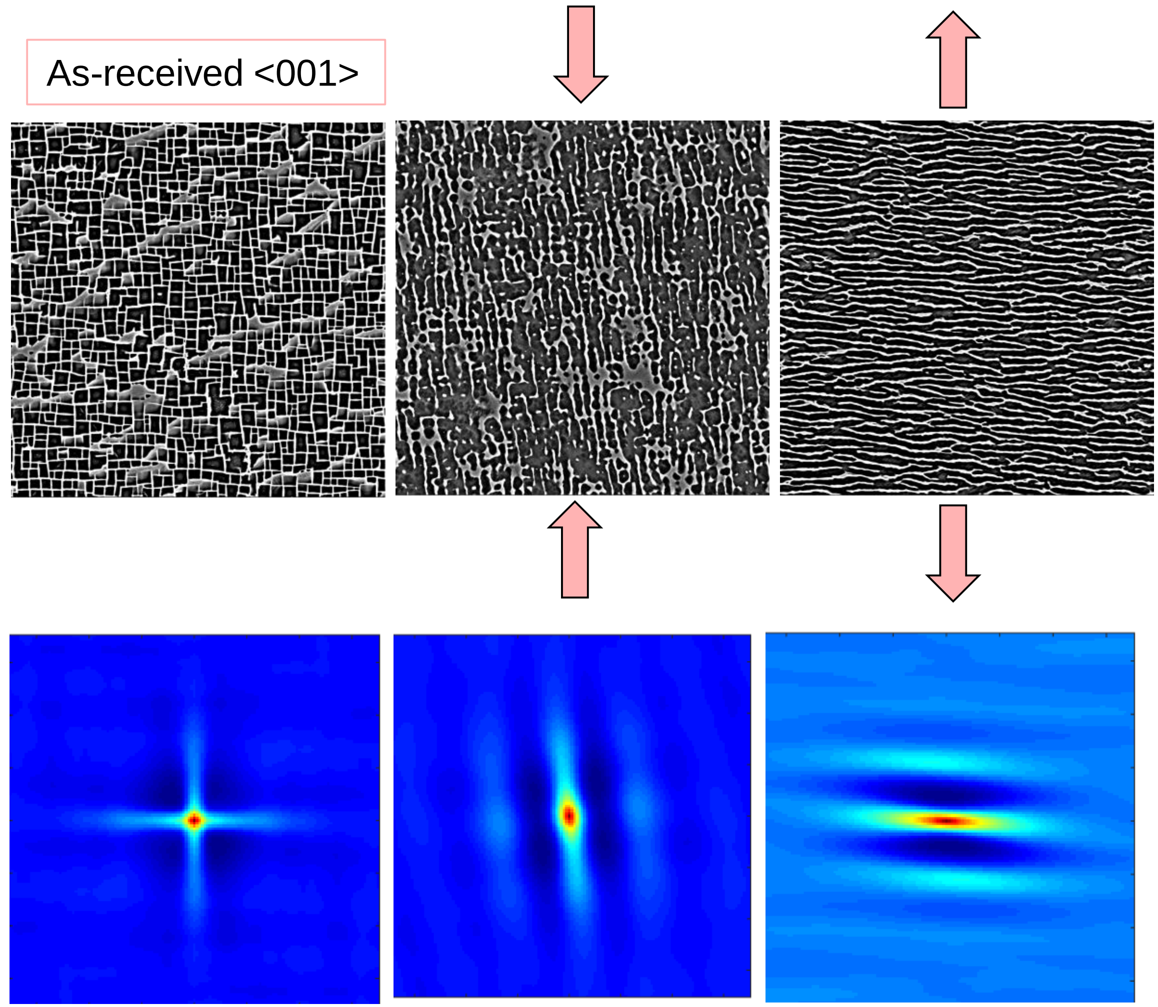

Large Dimensional Dataset generated by 2-point statistical spatial correlation

Data Visualization of Aged CMSX-8 in PC Space

- Application of PCA to the high dimension 2-point spatial correlation results in a reduced-order representation of microstructure ensemble.
- The axes are ordered descendingly by the extent of variation each explain.
- PCA is a linear approach to dimensionality reduction by coordinate transform.
- The axes are defined by the directions of the highest variance
- Powerful classification and visualization tool:
  Micrographs with similar microstructures are grouped in PC space automatically. The ones with significant different structures are located far from each other

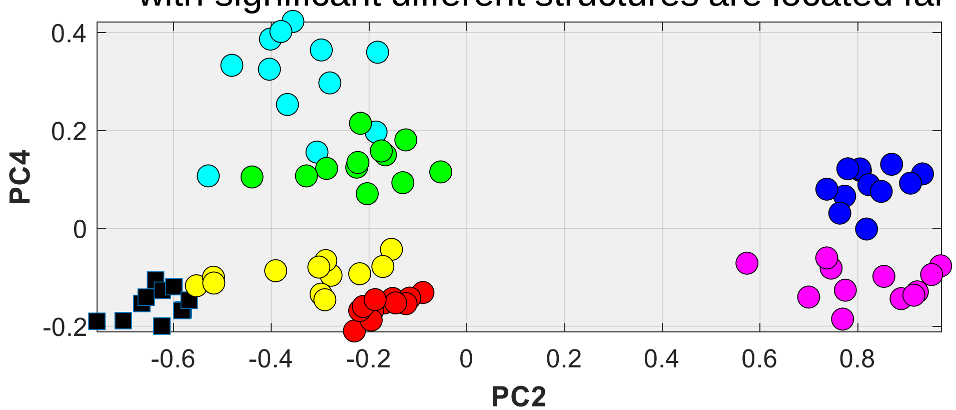

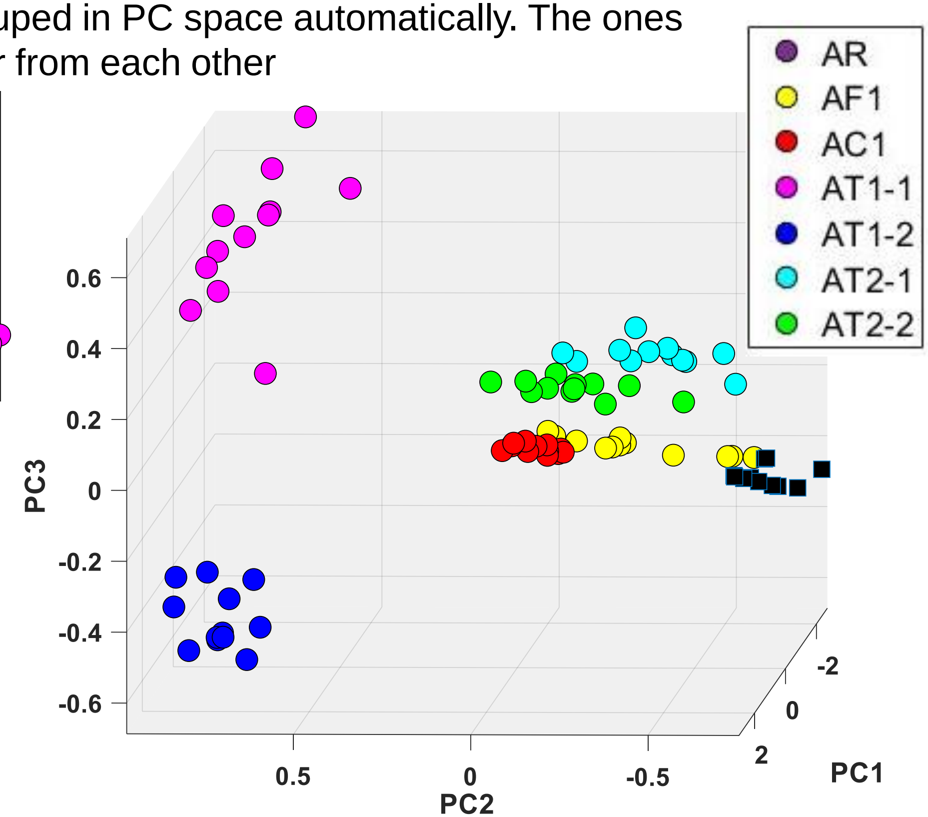

Sample ID	Temperature [˚C]	Stress [MPa] (min, max)	Dwell time (h)
AR	23	0	0
AT1-1	1120	95	50
AT1-2	1120	30	50
AT2-1	950	206	450
AT2-2	950	112	450
AC1	900	-208	850
AF1	950	0	940

Effect of Aging on Creep-Fatigue

Initial as-heat-treated microstructure

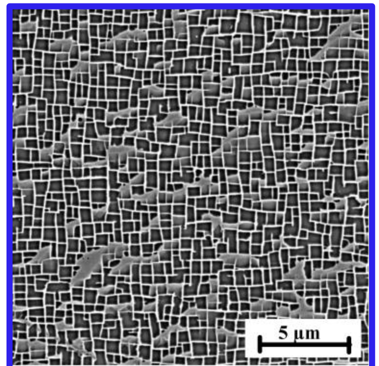

Pre-Aging

$\sigma = 130\ MPa,$

$T = 1100\ °C,$

$t = 50 - 60\ hours$

$\varepsilon_{creep} < 2\ \%$

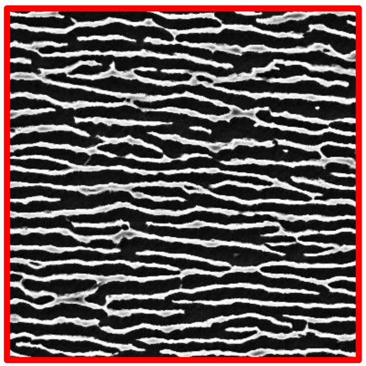

Removal of Oxide and γ' depleted zone

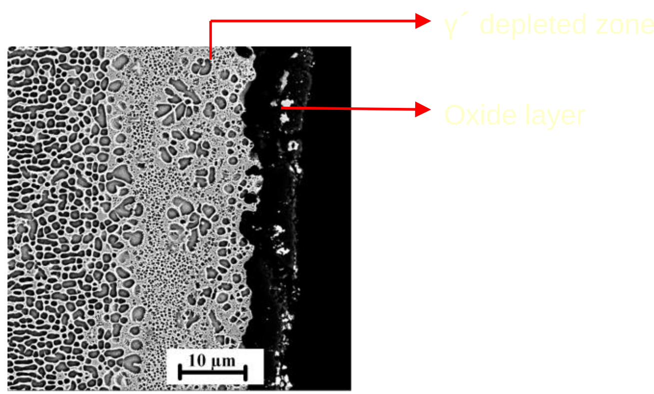

Pre-Creeping

$\sigma = 392\ MPa,$

$T = 900\ °C,$

$\varepsilon = 5 - 6\ \%$

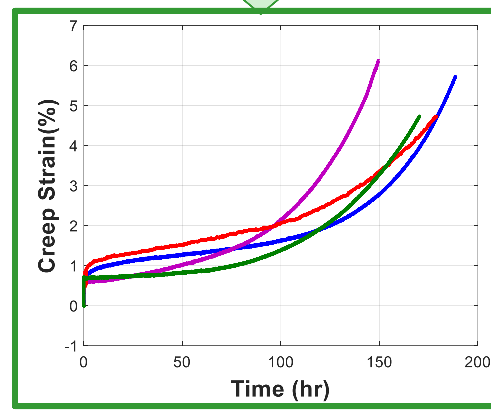

Removal of Oxide and γ' depleted zone

Role of Microstructure on LCF – Three Critical Temperature Regimes to Study

Room Temperature

- The primary mechanism is the dislocation ribbons shearing through the γ́ precipitates

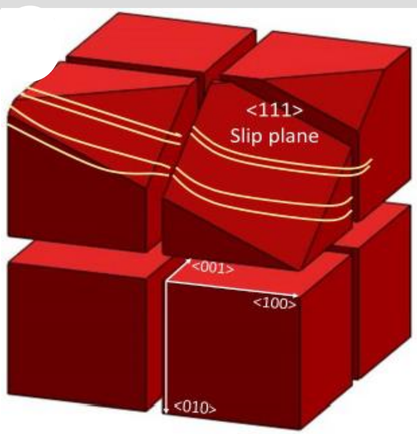

750 ° C

- Material exhibits its highest strength at this temperature

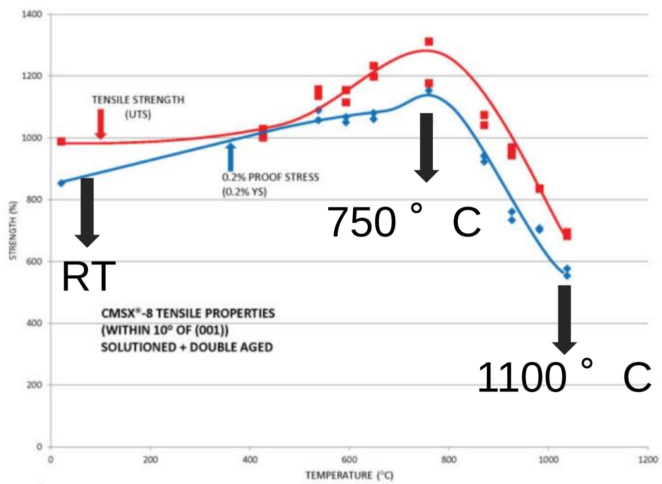

1100 ° C

- The dominated mechanism is cross slip and thermally assisted glide and climb of dislocations in γ channels

Influence of Microstructure
$R_\varepsilon = 0$ versus $R_\varepsilon = -\infty$ at 1100 ˚C

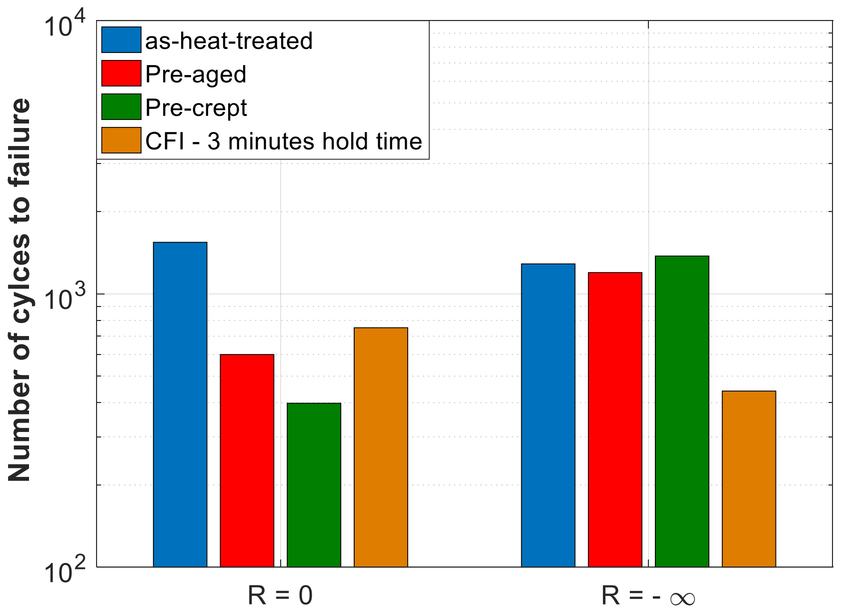

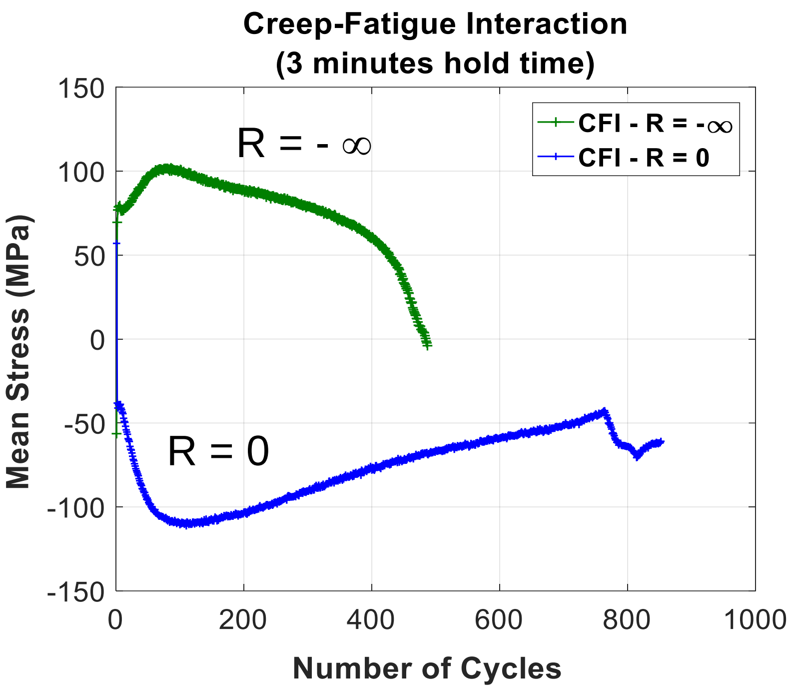

No notable microstructure influence when $R_\varepsilon = -\infty$.

Fatigue-environment interaction likely explanation when $R_\varepsilon = -\infty$.

Fracture surface topology – Low cycle fatigue at 1100° C

$\boldsymbol{R_\varepsilon = 0}$

As-heat-treated	Pre-aged	Pre-crept

$N_f = 1545$

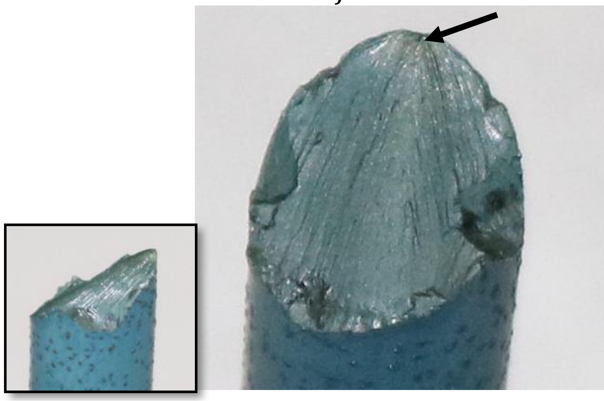

$N_f = 600$

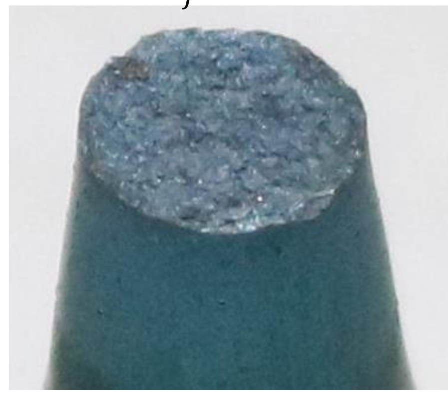

Necking: 20% reduction in area at fractured point

$N_f = 398$

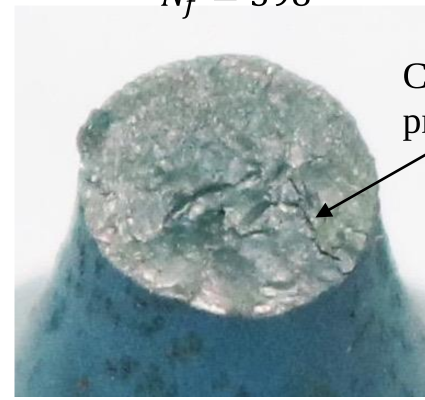

Necking: 25% reduction in area at fractured point

$\boldsymbol{R_\varepsilon = -\infty}$

$N_f = 1288$

$N_f = 1197$

$N_f = 1376$

Low Cycle Fatigue Response of CMSX-8 [001]
$R_\varepsilon = 0$, strain rate = 1×10^{-3} 1/s

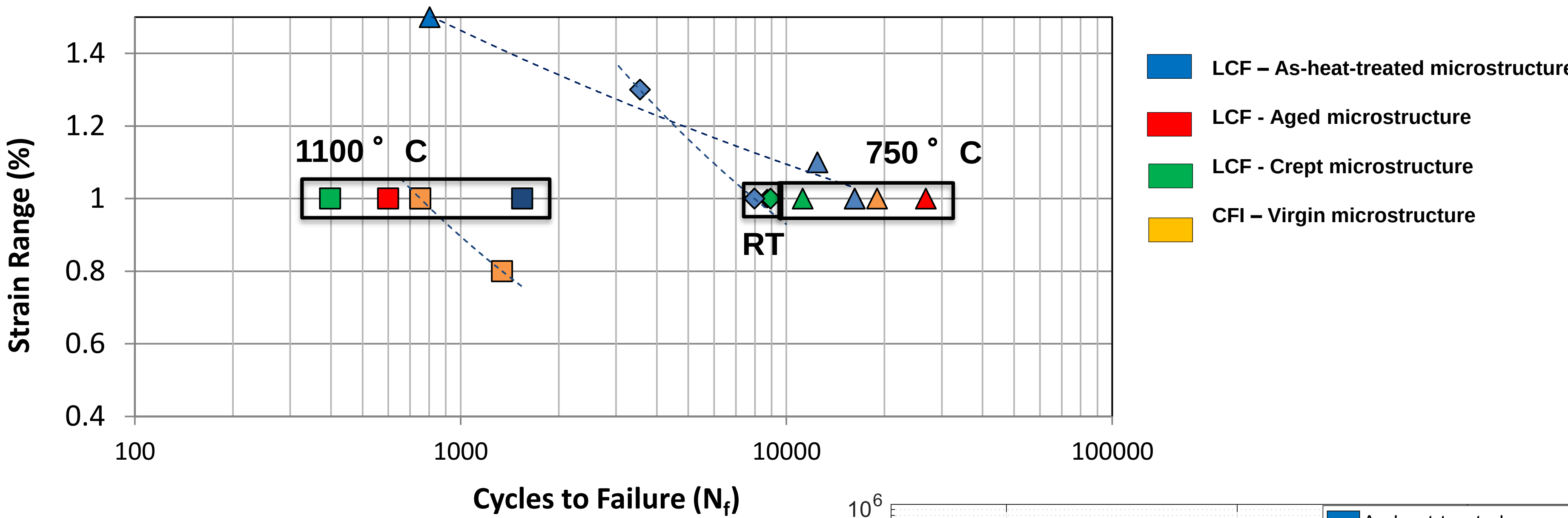

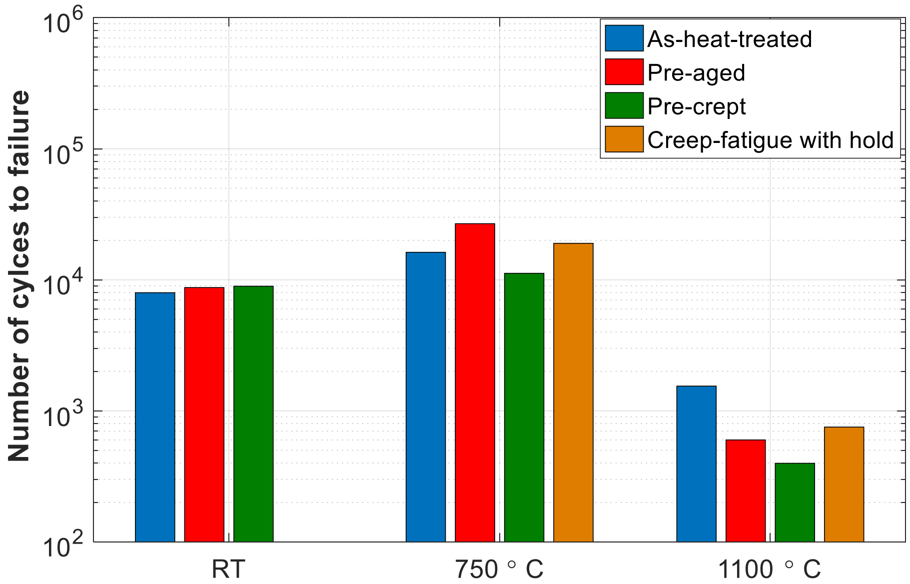

Only observe significant influence of microstructure on LCF at 1100° C

First 10 cycles – RT and 750 ˚C

RT

Elastic dominated cyclic response

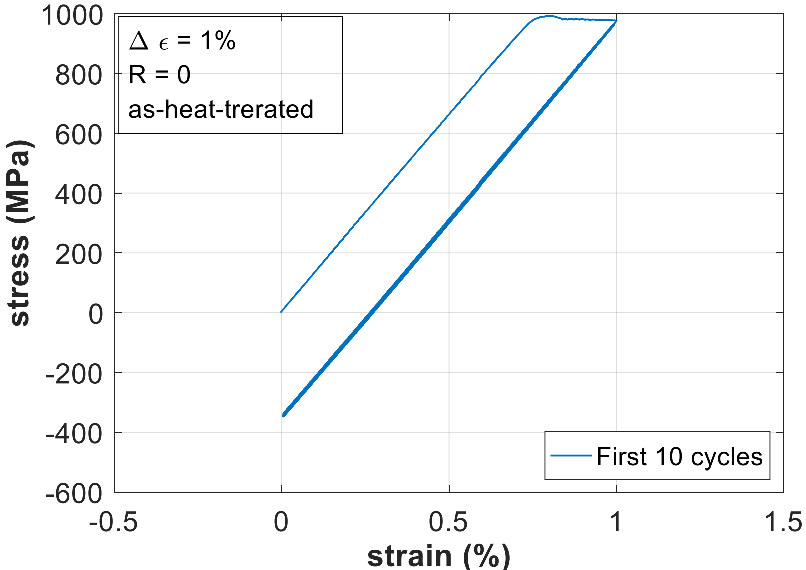

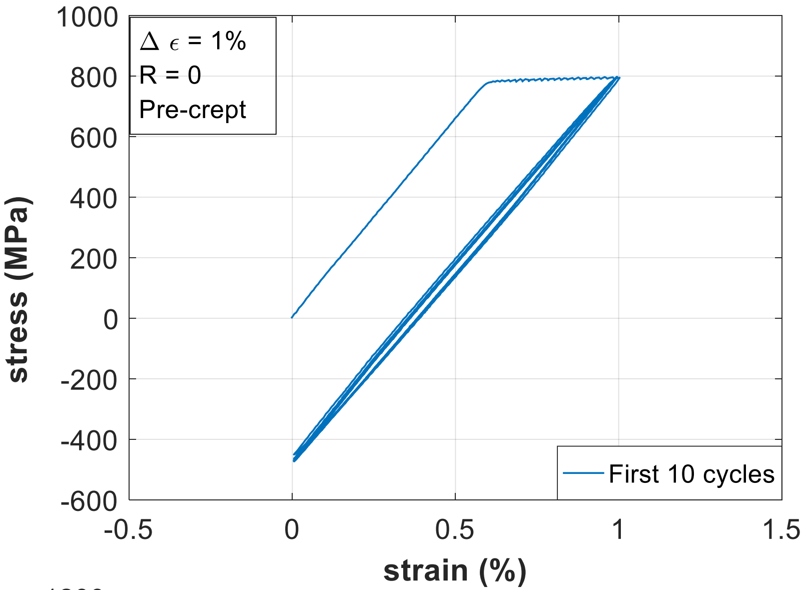

750 ° C

Elastic dominated cyclic response - *Peak strength*

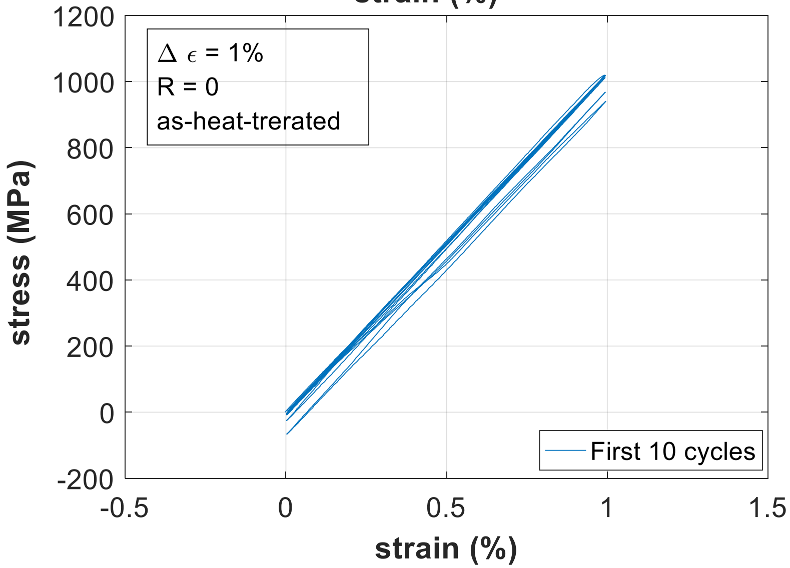

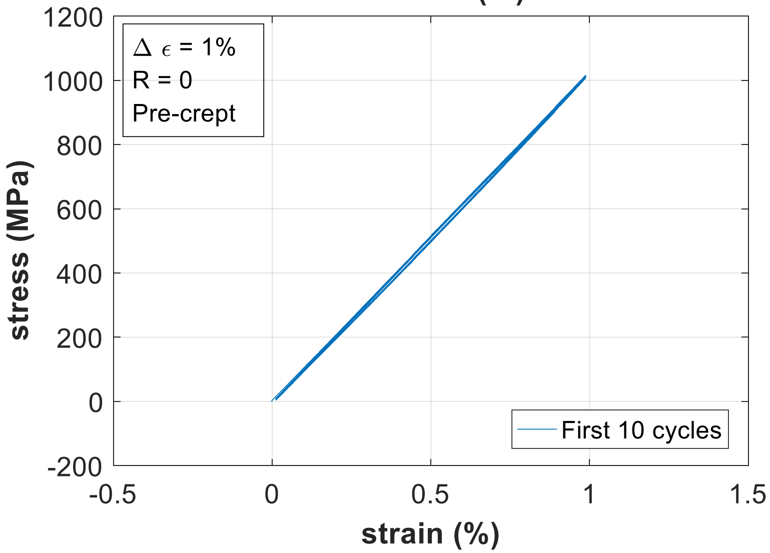

Fracture Surfaces

Low Cycle Fatigue at **Room Temperature**

As-heat-treated

Pre-crept

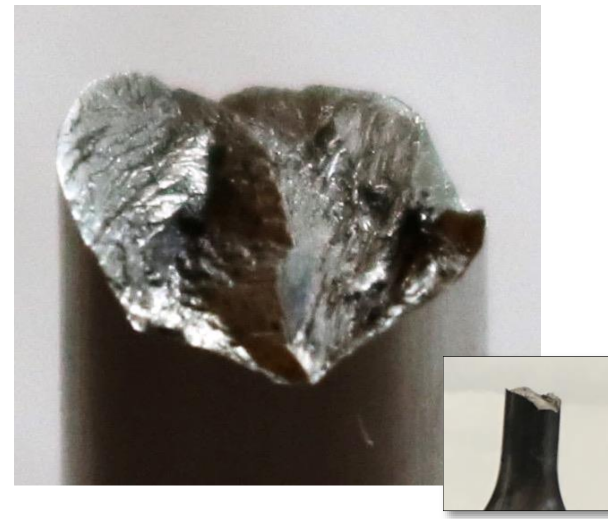

Low Cycle Fatigue at **750 ° C**

As-heat-treated

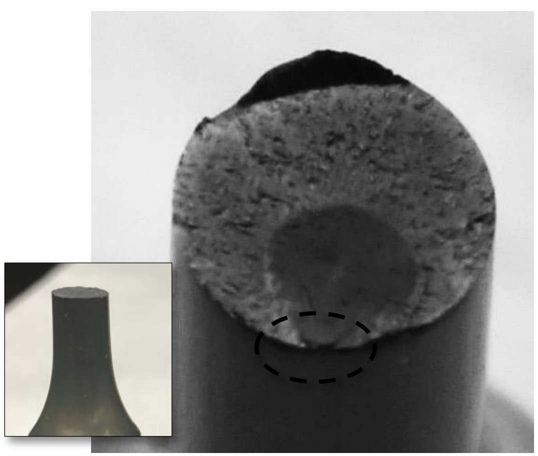

Pre-aged

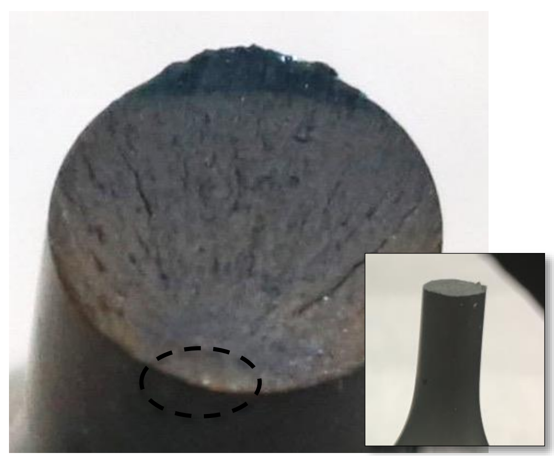

Pre-crept

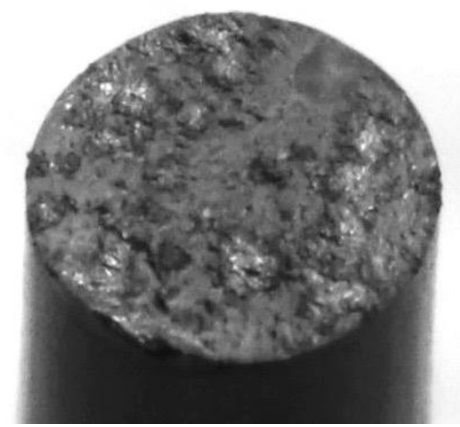

Crack Propagation Paths

LCF at **Room temperature**

Pre-aged microstructure

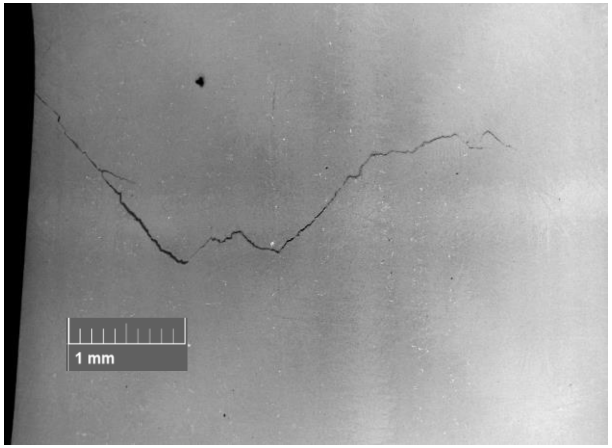

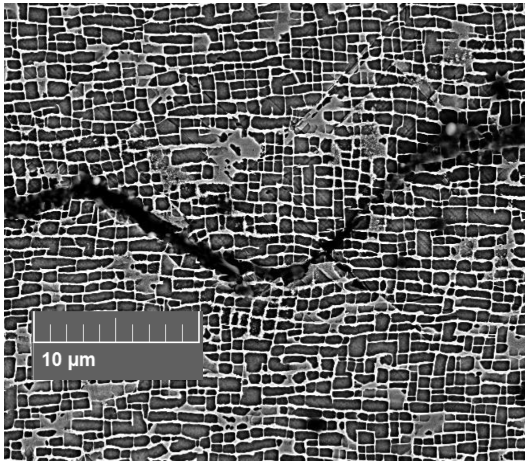

CFI at **750 ˚C**

As –heat – treated microstructure

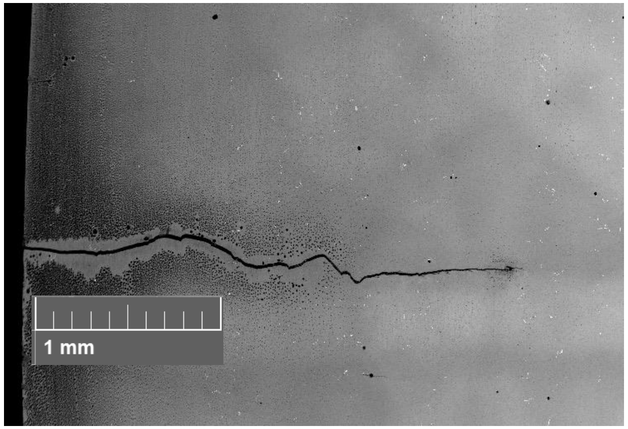

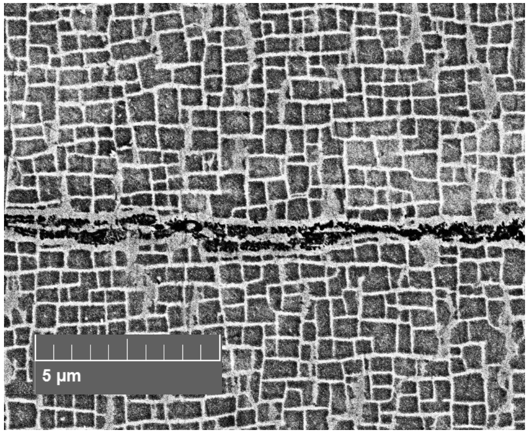

Primary Objectives of UTSR Project

- Creep-fatigue interaction experiments on CMSX-8
- Influence of aging on microstructure and creep-fatigue interactions
- Microstructure-sensitive, temperature-dependent crystal viscoplasticity to capture the creep and cyclic deformation response

Creep Deformation REGIMES

Microstructure Evolution Dominant Regime

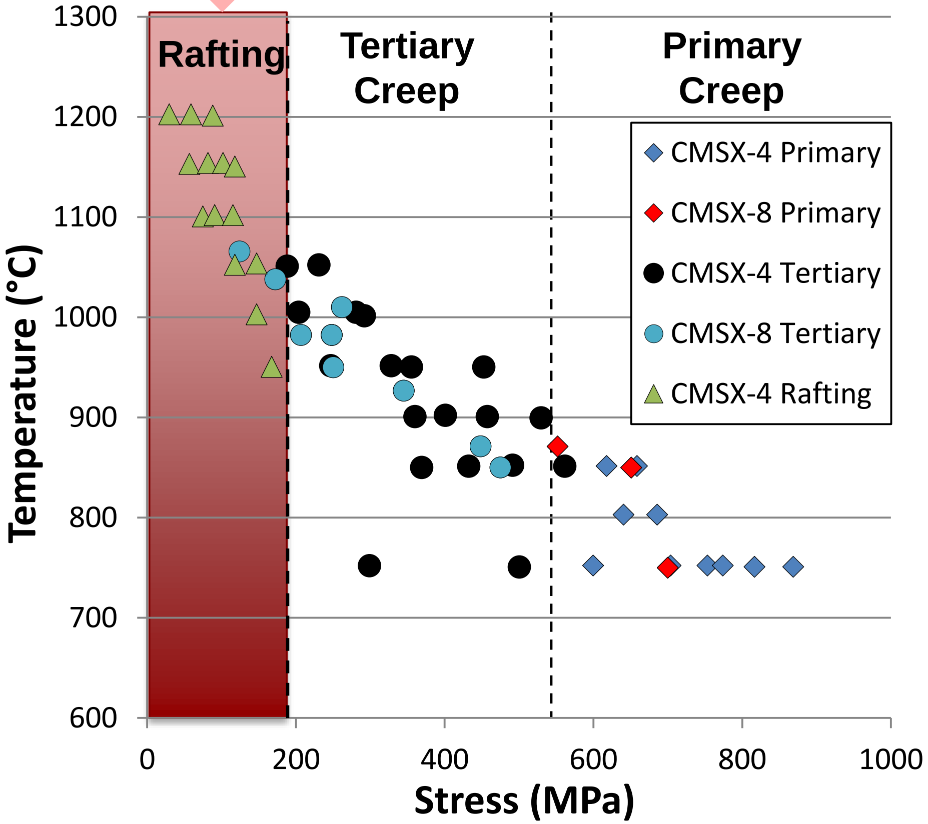

[Reed, 2006; Ma, Dye, and Reed, 2008; our CMSX-8 Data]

Tertiary – dislocation activity restricted to a/2<110> form operating on {111} slip planes in the γ channels

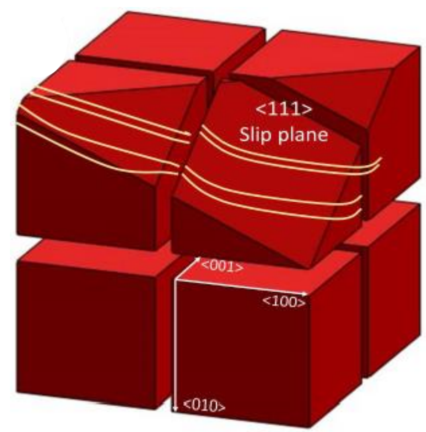

Primary – γ' particles are sheared by dislocation ribbons of overall Burgers vector a<112> dissociated into superlattice partial dislocations separated by a stacking fault; shear stress must above threshold stress (about 550 MPa)

Georgia Institute of Technology

Microstructure-sensitive Crystal Viscoplasticity for Single-Crystal Ni-base Superalloys

The George W. Woodruff School of Mechanical Engineering

School of Materials Science and Engineering

Alloy structure

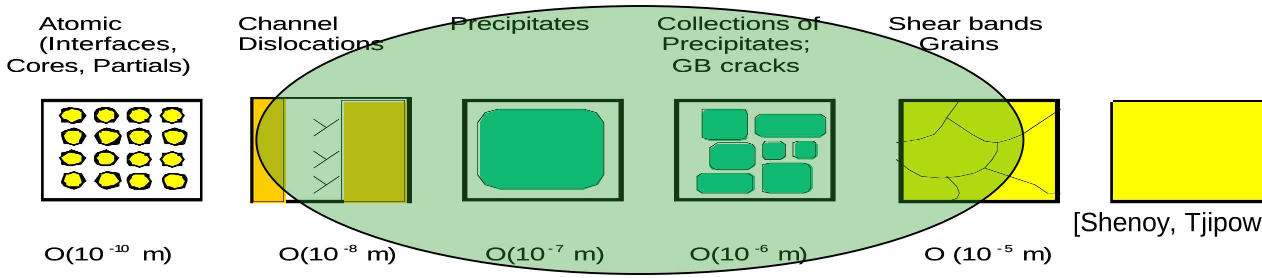

[Shenoy, Tjipowidjojo, and McDowell, 2008]

+

γ deformation

In γ : 12 octahedral slip systems active

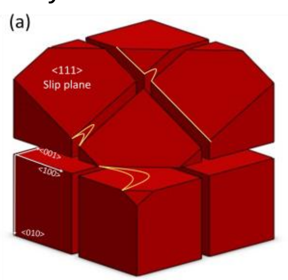

γ' deformation

In γ': 12 octahedral slip systems moving as dislocation ribbons

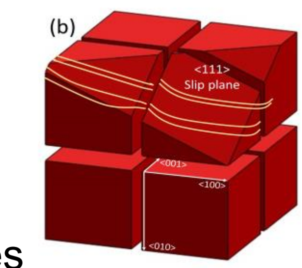

Distinct deformation in the γ and γ' phases

$$\mathbf{L}^{in} = f_{\gamma}\left(\sum_{\alpha=1}^{12}\dot{\gamma}_{\gamma}^{in(\alpha)}\left(\hat{\mathbf{d}}^{(\alpha)}\otimes\hat{\mathbf{n}}^{(\alpha)}\right)\right)+f_{\gamma'}\left(\sum_{\alpha=13}^{24}\dot{\gamma}_{L1_2}^{in(\alpha)}\left(\hat{\mathbf{d}}^{(\alpha)}\otimes\hat{\mathbf{n}}^{(\alpha)}\right)\right)$$

+

Deformation predictions sensitive to the γ and γ' phase attributes

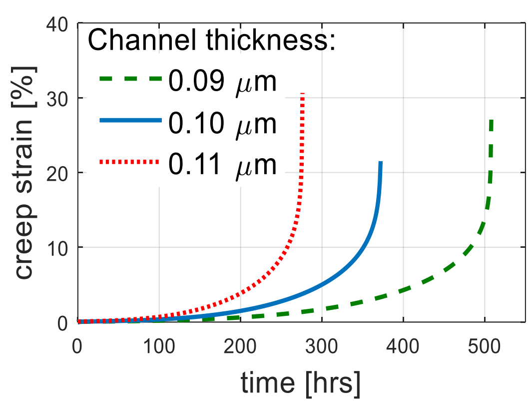

Tertiary creep: 950 °C, Stress = 400 MPa

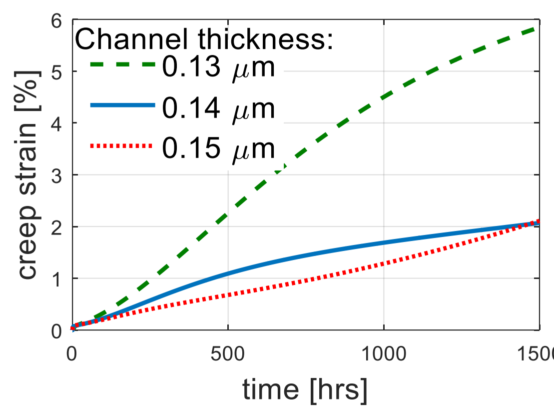

Primary creep: 750 °C, Stress = 680 MPa

Crystal Viscoplasticity – Kinematic Relations

Kinematic relations including temperature dependence

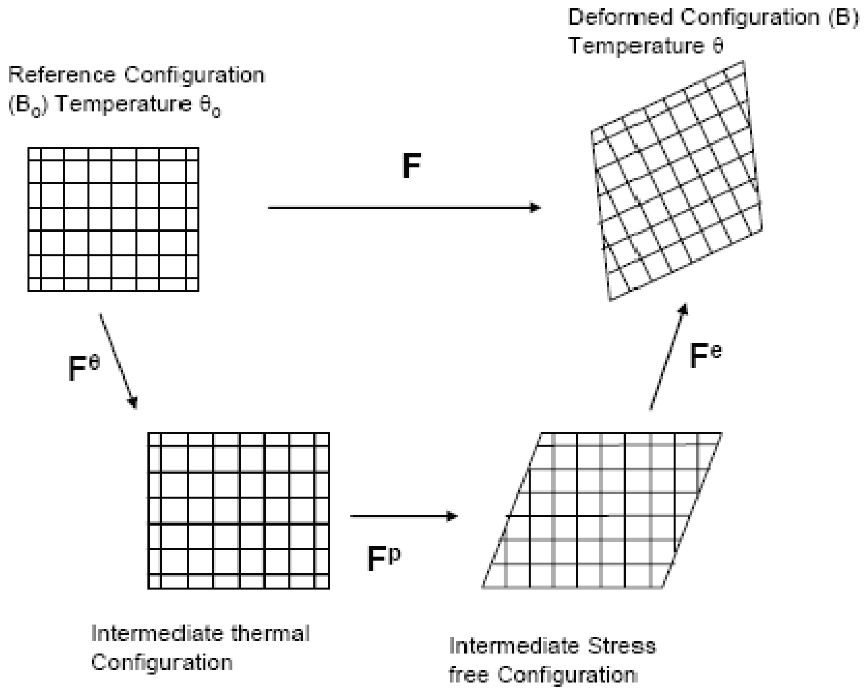

Deformation gradient

$$\mathbf{F} = \frac{\partial \mathbf{x}}{\partial \mathbf{X}} = \mathbf{F}^e \cdot \mathbf{F}^p \cdot \mathbf{F}^\theta$$

Velocity gradient

$$\mathbf{L} = \dot{\mathbf{F}} \cdot \mathbf{F}^{-1}$$

Macroscopic plastic velocity gradient

$$\mathbf{L}^p = \dot{\mathbf{F}}^p\, \mathbf{F}^{p^{-1}} = \sum_{\alpha=1}^{N_{slip}} \dot{\gamma}^{(\alpha)} \left(\mathbf{s}_o^{(\alpha)} \otimes \mathbf{n}_o^{(\alpha)} \right)$$

In γ : 12 octahedral slip systems active

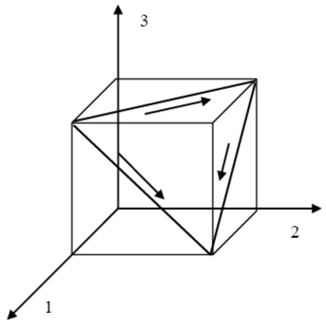

In γ': 12 octahedral slip systems moving as dislocation ribbons

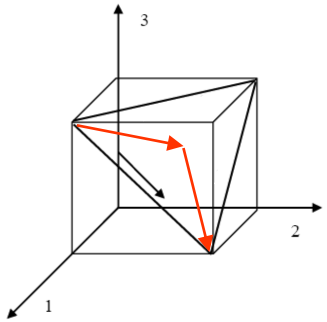

Crystal Viscoplasticity (CVP) – Rate Eqn

Inelastic Velocity Gradient

$$\mathbf{L}^{in} = \dot{\mathbf{F}}^{in}\mathbf{F}^{in^{-1}} = f_\gamma\left(\sum_{\alpha=1}^{12}\dot{\gamma}_\gamma^{in(\alpha)}\left(\hat{\mathbf{d}}^{(\alpha)}\otimes\hat{\mathbf{n}}^{(\alpha)}\right)\right) + f_{\gamma'}\left(\sum_{\alpha=13}^{24}\dot{\gamma}_{L1_2}^{in(\alpha)}\left(\hat{\mathbf{d}}^{(\alpha)}\otimes\hat{\mathbf{n}}^{(\alpha)}\right)\right)$$

Inelastic Shear Strain Rate

$$\begin{cases}\dot{\gamma}_\gamma^{in(\alpha)} = \rho^{(\alpha)}_\gamma\, b\,\lambda_\gamma^{(\alpha)} F_{attack}\, sign\left(\tau^{(\alpha)}+\tau^{(\alpha)}_{mis}-\chi^{(\alpha)}\right)\exp\left\{\dfrac{-Q_{slip}^{110}+\left(\left|\tau^{(\alpha)}+\tau^{(\alpha)}_{mis}-\chi^{(\alpha)}\right|-\tau^{(\alpha)}_{\gamma pass}-\tau^{(\alpha)}_{oro}\right)V_{c1}^{(\alpha)}}{kT}\right\} \\ \dot{\gamma}_{L1_2}^{in(\alpha)} = \rho_{L1_2}^{(\alpha)} b\,\lambda_{L1_2}^{(\alpha)} F_{attack}\, sign\left(\tau^{(\alpha)}-\chi^{(\alpha)}\right)\exp\left\{\dfrac{-Q_{slip}^{112}+\left(\left|\tau^{(\alpha)}-\chi^{(\alpha)}\right|-\tau^{(\alpha)}_{L1_2 pass}-\tau_{APB}\right)V_{c2}^{(\alpha)}}{kT}\right\}\end{cases}$$

Dislocation Density Evolution Equations

$$\begin{cases}\dot{\rho}_\gamma^{(\alpha)} = \dfrac{1}{b}\left(\dfrac{c_{mult1}}{\lambda_\gamma^{(\alpha)}} - c_{annh1}\rho_\gamma^{(\alpha)}\right)\left|\dot{\gamma}_\gamma^{in(\alpha)}\right| \\ \dot{\rho}_{L1_2}^{(\alpha)} = c_{mult21}\rho_{pb}^{(\alpha)}\Gamma + \dfrac{c_{mult22}}{b\lambda_{\gamma'}^{(\alpha)}}\left|\dot{\gamma}_{\gamma'}^{(\alpha)}\right| - c_{annh2}\rho_{\gamma'}^{(\alpha)}\left|\dot{\gamma}_{\gamma'}^{(\alpha)}\right| \\ \dot{\rho}_{pb}^{(\alpha)} = \dfrac{c_{mult}^{pb}}{bL_\gamma}\left|\dot{\gamma}_\gamma^{in(\alpha)}\right| - c_{annh}^{pb}\rho_{pb}^{(\alpha)}\left|\dot{\gamma}_\gamma^{in(\alpha)}\right|\end{cases}$$

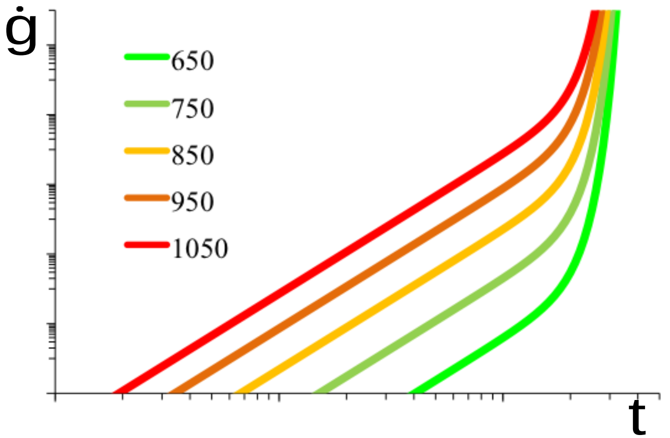

Evolution of dislocation densities

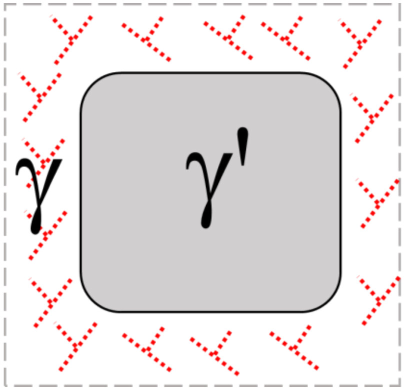

$$\dot{\rho}_{\gamma}^{(\alpha)} = \frac{1}{b}\left(\overbrace{\frac{c_{mult1}}{\lambda_{\gamma}^{(\alpha)}}}^{\text{multiplication}} \overbrace{- c_{annh1}\rho_{\gamma}^{(\alpha)}}^{\text{annihilation}}\right)\left|\dot{\gamma}_{\gamma}^{in(\alpha)}\right|$$

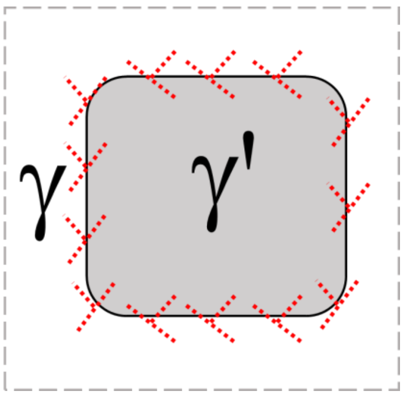

$$\dot{\rho}_{pb}^{(\alpha)} = \frac{c_{mult}^{pb}}{bL_{\gamma}}\left|\dot{\gamma}_{\gamma}^{in(\alpha)}\right| - c_{annh}^{pb}\rho_{pb}^{(\alpha)}\left|\dot{\gamma}_{\gamma}^{in(\alpha)}\right|$$

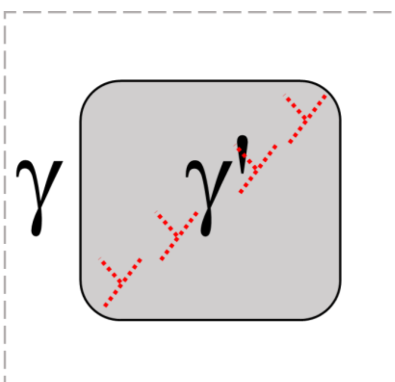

$$\dot{\rho}_{L1_2}^{(\alpha)} = c_{mult21}\rho_{pb}^{(\alpha)}\Gamma + \frac{c_{mult22}}{b\lambda_{\gamma'}^{(\alpha)}}\left|\dot{\gamma}_{\gamma'}^{(\alpha)}\right| - c_{annh2}\rho_{\gamma'}^{(\alpha)}\left|\dot{\gamma}_{\gamma'}^{(\alpha)}\right|$$

Creep in different orientations

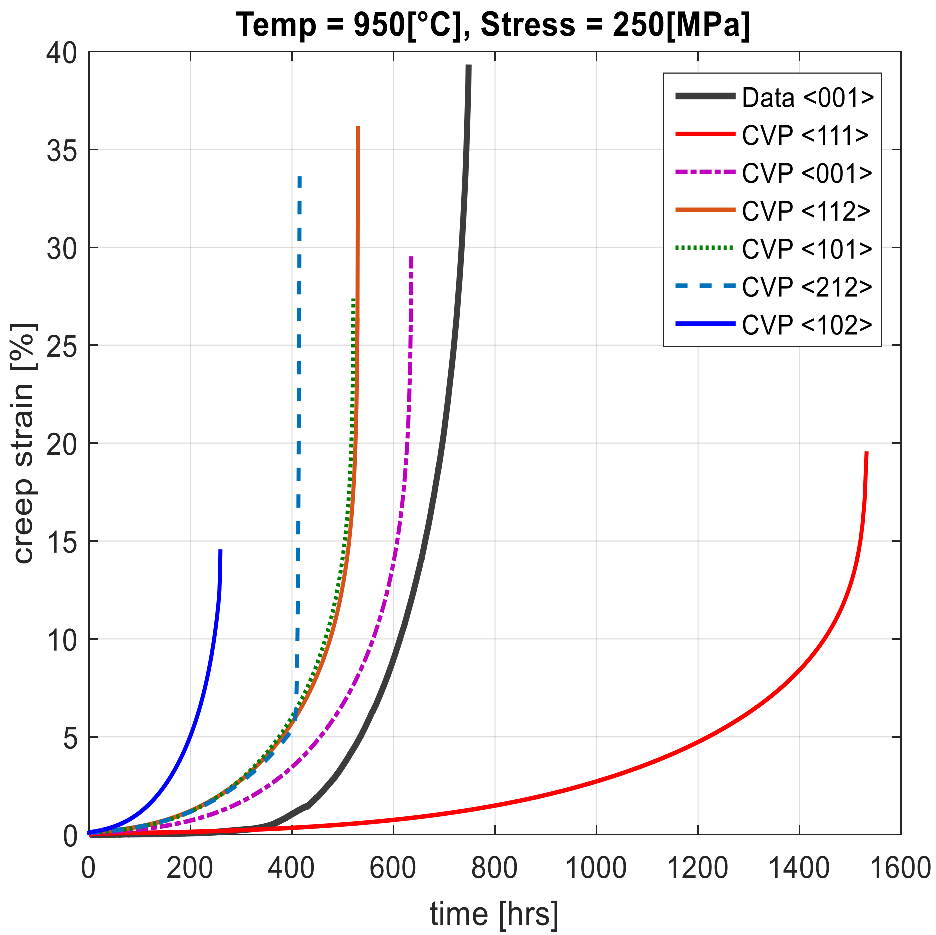

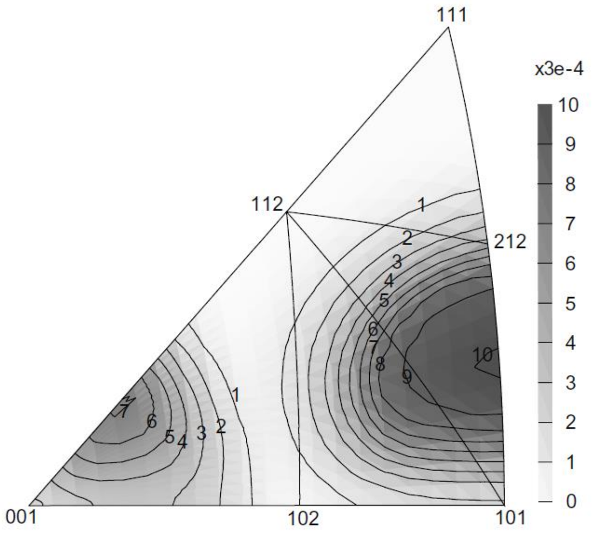

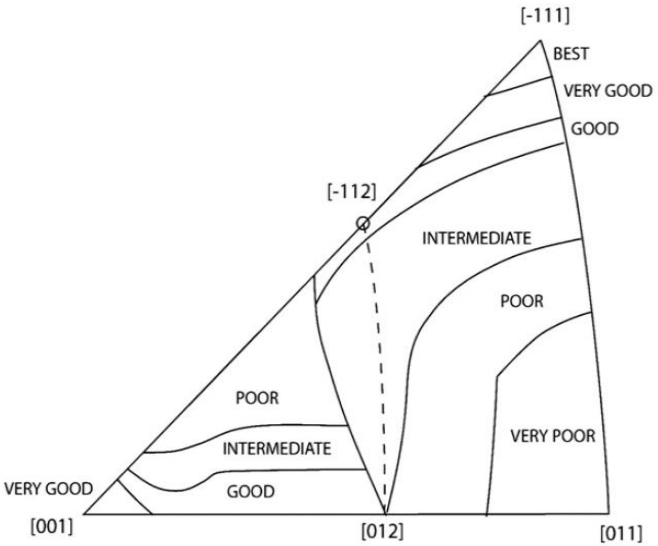

Various Creep Predictions

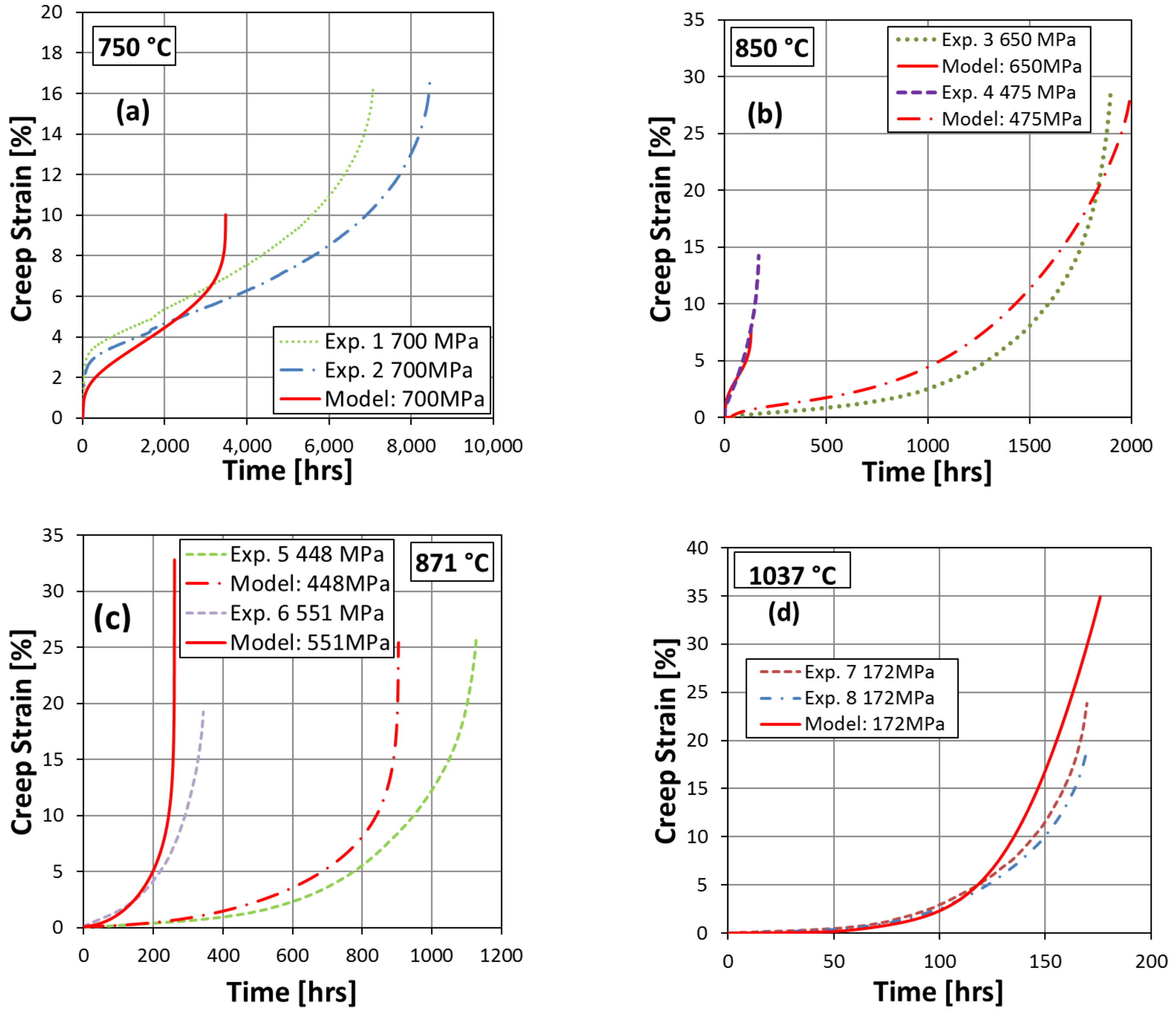

Effect of Channel Size on Creep

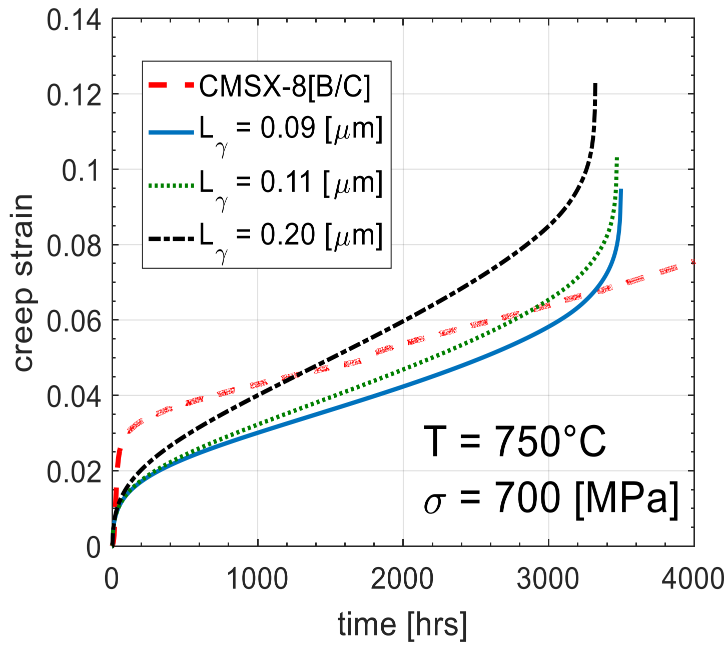

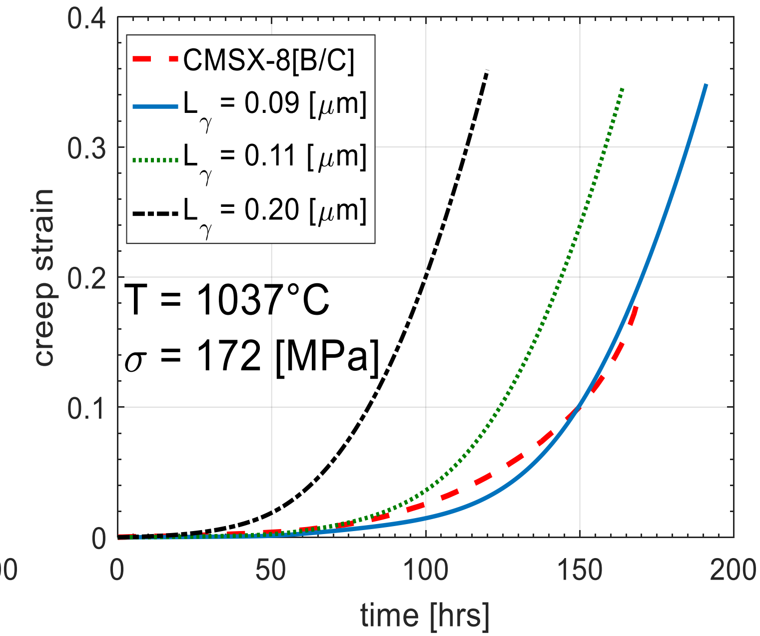

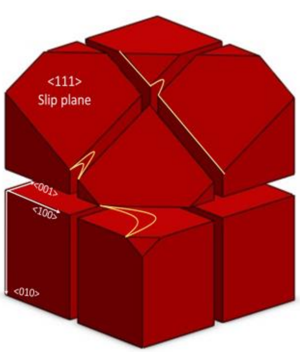

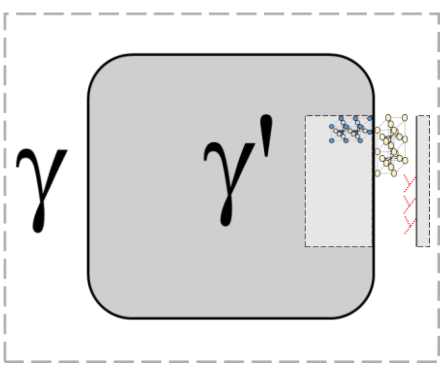

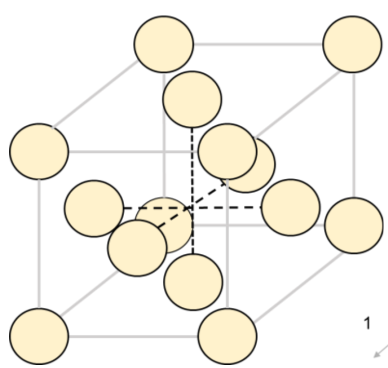

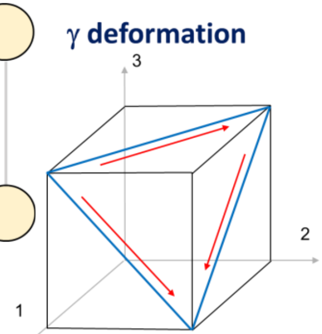

Effect of APB Energy on Creep

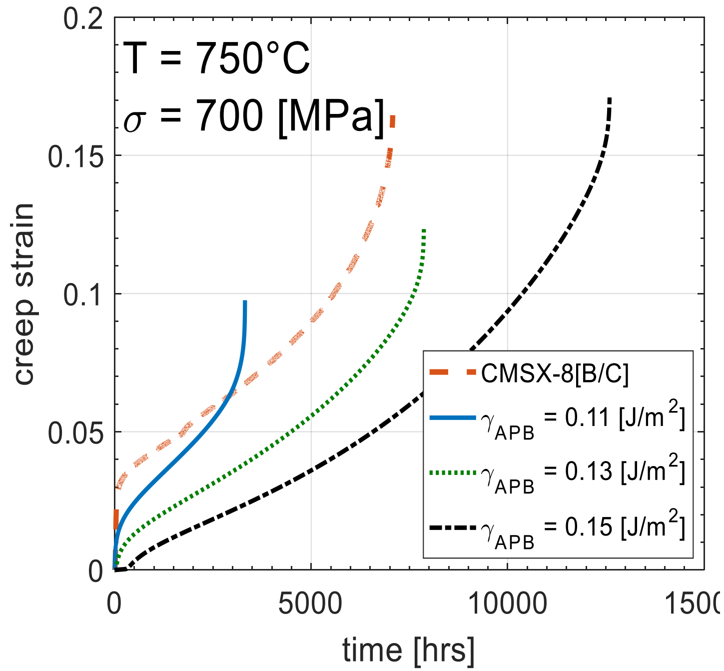

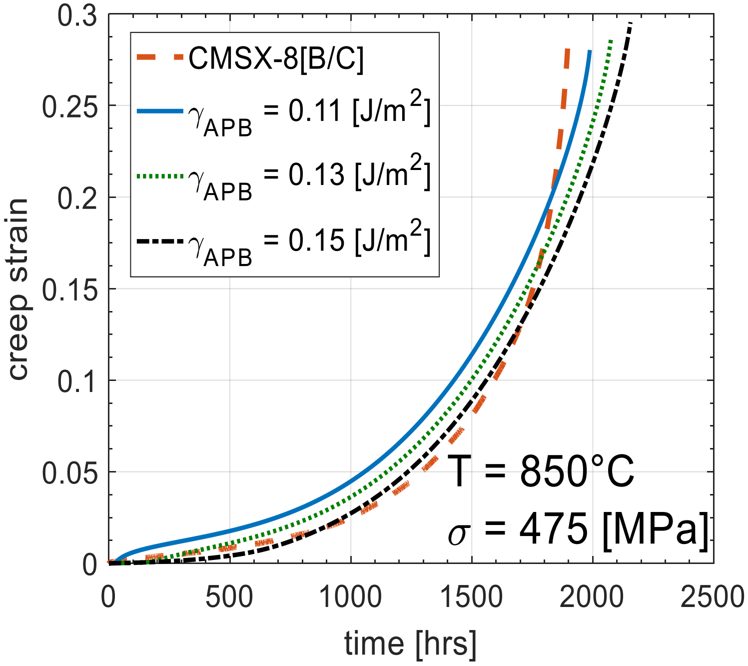

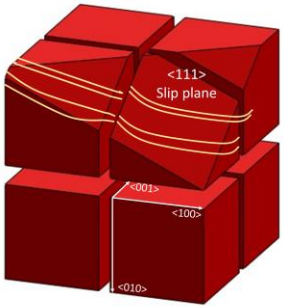

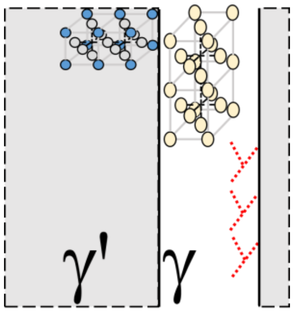

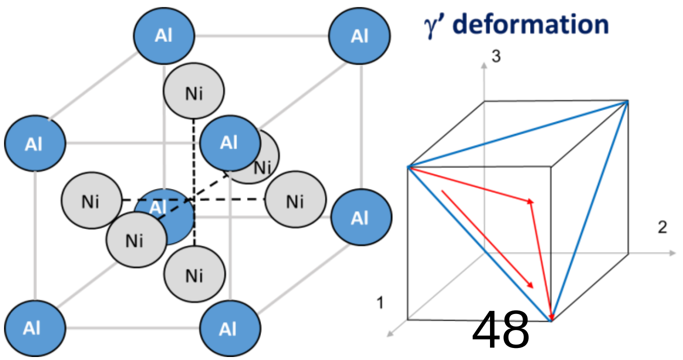

Primary and Tertiary Creep

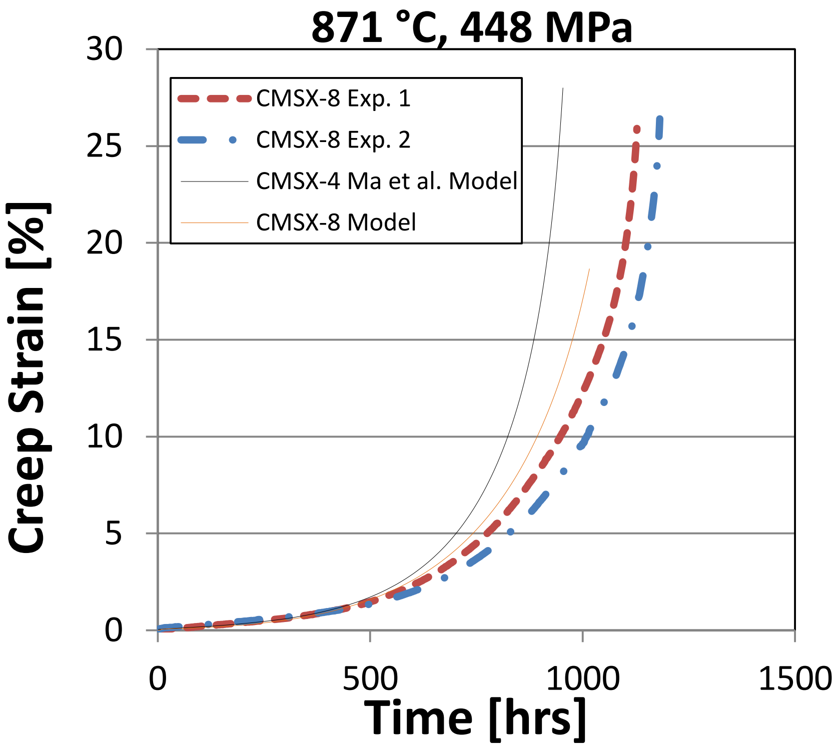

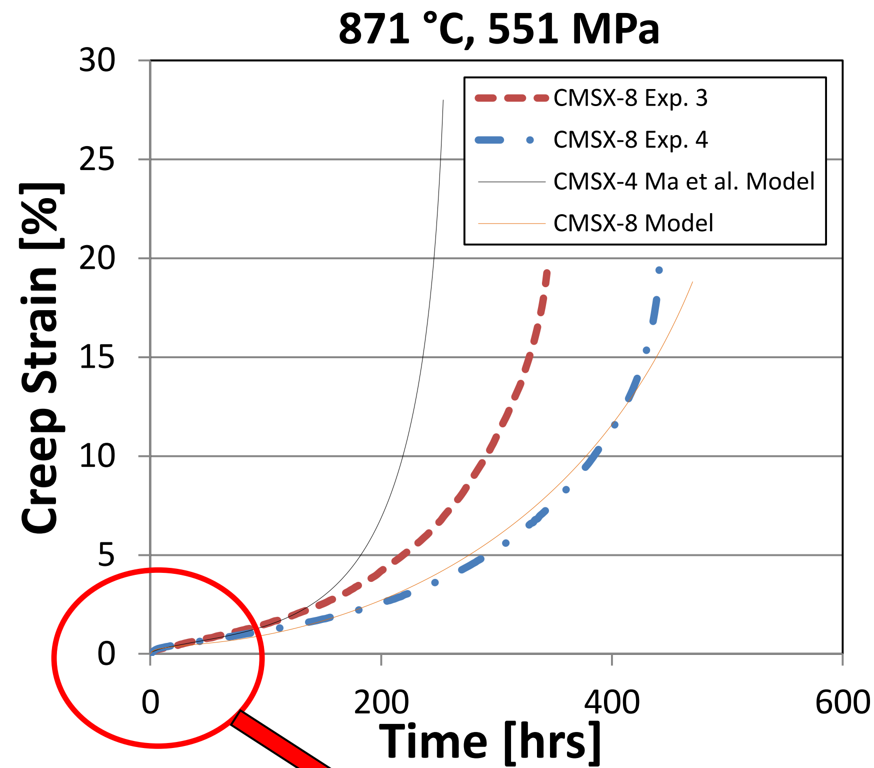

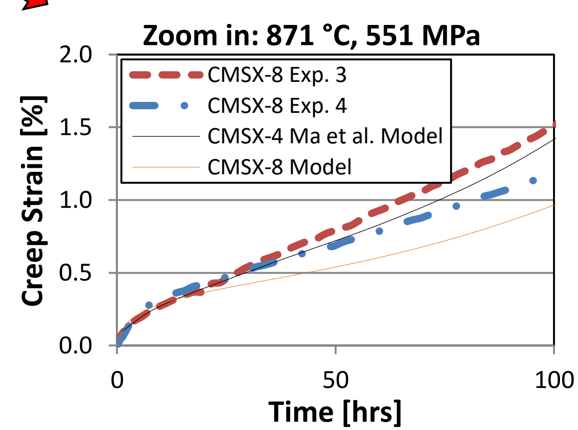

Primary, secondary and tertiary creep can be captured with the model

TMF validation

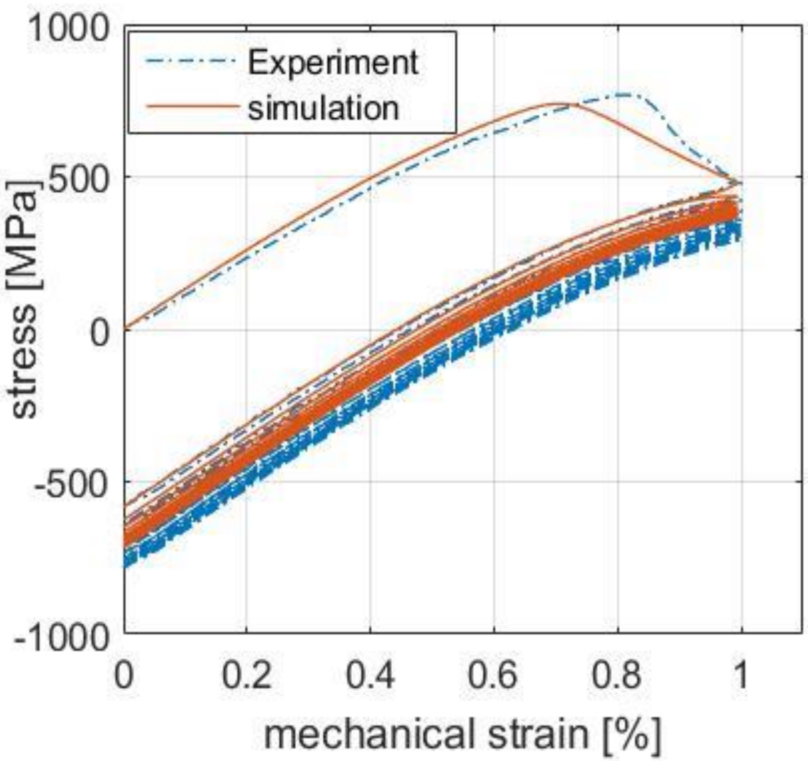

First 10 cycles: IP-TMF
[100-1100-100] ºC, R = 0, $\dot{T} = 2.83[°K/s]$

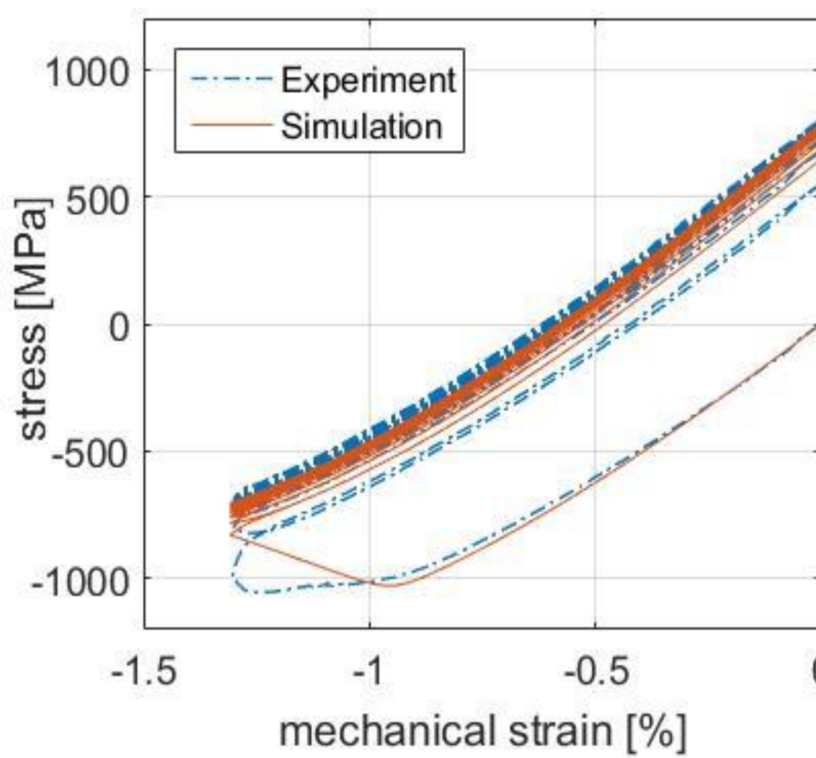

Stabilized hysteresis: OP-TMF
[100-850-100] ºC, R = -∞, $\dot{T} = 2.83[°K/s]$

Very good agreement predicting TMF

Incorporating the Influence of Re Content

Since Re segregates almost exclusively in the γ channels, the Activation energy in the γ phase can be modified to account for Re content as follows:

$$\begin{cases} \dot{\gamma}_{\gamma}^{in(\alpha)} = \Theta(T)\,\rho^{(\alpha)}_{\gamma}\, b\, \lambda^{(\alpha)}_{\gamma} F_{attack}\, sign\left(\tau^{(\alpha)} + \tau^{(\alpha)}_{mis} - \chi^{(\alpha)}\right) \exp\left\{ \dfrac{-Q^{110}_{slip} + \left(\left| \tau^{(\alpha)} + \tau^{(\alpha)}_{mis} - \chi^{(\alpha)} \right| - \tau^{(\alpha)}_{\gamma pass} - \tau^{(\alpha)}_{oro} \right) V^{(\alpha)}_{c1}}{kT} \right\} \\ \dot{\gamma}_{L1_2}^{in(\alpha)} = \rho^{(\alpha)}_{L1_2}\, b\, \lambda^{(\alpha)}_{L1_2} F_{attack}\, sign\left(\tau^{(\alpha)} - \chi^{(\alpha)}\right) \exp\left\{ \dfrac{-Q^{112}_{slip} + \left(\left| \tau^{(\alpha)} - \chi^{(\alpha)} \right| - \tau^{(\alpha)}_{L1_2 pass} - \tau_{APB} \right) V^{(\alpha)}_{c2}}{kT} \right\} \end{cases}$$

If we considering activation energy for plastic flow Q_0 a function of %Re, the diffusivity parameter could take the form of:

$$\Theta(T) = \exp\left(-\frac{Q_o}{RT} \right) \quad \text{for } T \geq \frac{T_m}{2} \qquad\qquad \mathrm{Q}(T) = \exp\left(-\frac{2Q_o}{RT} \left[\ln\left(\frac{T_m}{2T} \right) + 1 \right] \right) \quad \text{for } T \leq \frac{T_m}{2}$$

[Miller, 1976; Shenoy et al., 2005]

Intellectual Impacts

Georgia Institute of Technology

The George W. Woodruff School of Mechanical Engineering | School of Materials Science and Engineering

Creep-Fatigue Interaction Experiments and Lifetime Models

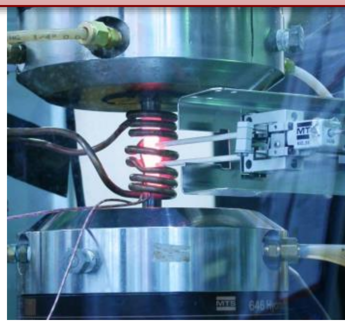

Microstructure-sensitive Crystal Viscoplasticity (CVP) Model to Determine Service "Process"-Structure-Property Linkages

$$\mathbf{L}^{in} = \dot{\mathbf{F}}^{in}\,\mathbf{F}^{in^{-1}} = f_\gamma\left(\sum_{\alpha=1}^{12}\dot{\gamma}_\gamma^{in(\alpha)}\left(\hat{\mathbf{d}}^{(\alpha)}\otimes\hat{\mathbf{n}}^{(\alpha)}\right)\right) + f_{\gamma'}\left(\sum_{\alpha=13}^{24}\dot{\gamma}_{L1_2}^{in(\alpha)}\left(\hat{\mathbf{d}}^{(\alpha)}\otimes\hat{\mathbf{n}}^{(\alpha)}\right)\right)$$

γ deformation

γ' deformation

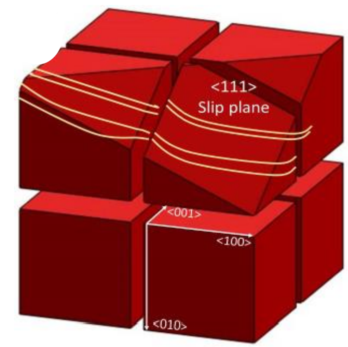

Experiments & Models (both physically-based and data analytics) to Predict Current State of Microstructure (Service Process-Structure Linkages)

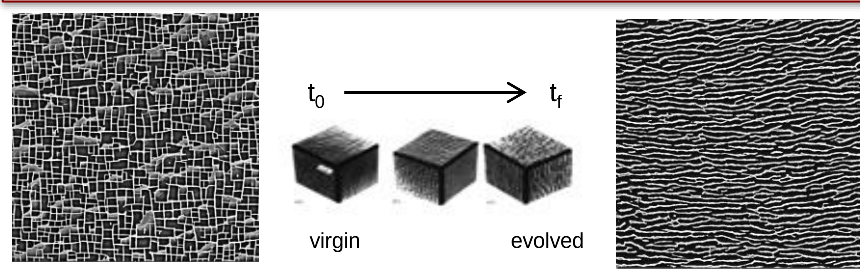

- Stress-free and stress-assisted (rafting) aging experiments under tensile and compressive stresses
- Establishing process-structure linkages using physical models, 2-point statistics and PCA

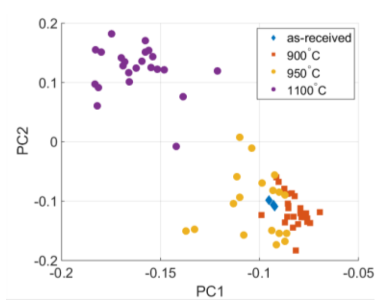

Established Method to Determine Sensitivity of Local Composition on Diffusivity for Input in Aging and Viscoplasticity Models

Thermo-Calc
DICTRA
Databases: TCNi5 / MOBNi2

Thermo-Calc Software

- Composition segregation in γ and γ' phase
- Determination of composition sensitive effective diffusivity to characterize aging activation energy and diffusivity parameter in viscoplasiticity models

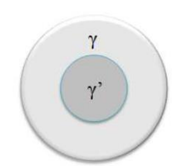

Acknowledgments

This work is supported by

UTSR
University Turbine Systems Research

Grant DE-FE0011722

SIEMENS
energy